Cretaceous Research 162 (2024) 105952

Contents lists available at ScienceDirect

Cretaceous Research

journal homepage: www.elsevier.com/locate/CretRes

Theropod teeth palaeodiversity from the uppermost Cretaceous of the South Pyrenean Basin (NE Iberia) and the intra-Maastrichtian faunal turnover

Erik Isasmendi [a, *], Manuel Pérez-Pueyo [b], Miguel Moreno-Azanza [b], Antonio Alonso [b], Eduardo Puértolas-Pascual [b], Beatriz Bádenas [b], José Ignacio Canudo [b]

[a] Departamento de Geología/Geologia Saila, Facultad de Ciencia y Tecnología/Zientzia eta Teknologia Fakultatea, Universidad del País Vasco/Euskal Herriko Unibertsitatea, 48940 Leioa, Spain
[b] Grupo Aragosaurus-IUCA, Facultad de Ciencias, Universidad de Zaragoza, 50009 Zaragoza, Spain

ARTICLE INFO

Article history:
Received 16 November 2023
Received in revised form
11 June 2024
Accepted in revised form 12 June 2024
Available online 17 June 2024

Keywords:
Abelisauridae
Coelurosauria
Theropoda
Maastrichtian
Pyrenees
Europe

ABSTRACT

The South Pyrenean Basin has yielded abundant dinosaur and penecontemporaneous vertebrate fossils, becoming one of the most important areas in Europe for the study of these faunas. The studied isolated theropod teeth from the Western Tremp Syncline (NE Iberia) were recovered from the uppermost Maastrichtian (topmost Arén and Tremp formations). The studies conducted have led to the identification of eight tooth morphotypes, which are referred to cf. *Paronychodon*, cf. *Richardoestesia*, an abelisaurid, a dromaeosaurid, and a non-dromaeosaurid paravian. Together with the previously reported troodontid and ornithuromorph, this study increases the known theropod palaeobiodiversity in the area to seven taxa. The latest Maastrichtian theropod fauna of the Western Tremp Syncline is thus composed of a medium to large-sized abelisaurid as well as a high diversity of small-bodied early-branching coelurosaurians and avialans, as seen in other Ibero-Armorican localities. Revision of the literature concerning the theropods of the Ibero-Armorican domain indicates that, although similar theropod groups were present before, during, and after the intra-Maastrichtian faunal turnover (an event constrained to between the early Maastrichtian and the early late Maastrichtian; lower part of C31r to the C30r/C30n reversal), there were changes in the abelisaurid, dromaeosaurid, and large avialan assemblages, as well as in the proportions of indeterminate paravian and cf. *Richardoestesia* morphotypes, with the presence of troodontids only recorded in post-turnover faunas. These changes suggest that theropods might have been affected by the turnover event. Nevertheless, further studies and more complete specimens could shed more light on the effects of this faunal turnover, and on the affinities and palaeobiodiversity of the latest Cretaceous Ibero-Armorican theropods.

1. Introduction

The European continent includes a particularly large number of fossil sites from the uppermost Cretaceous (Csiki-Sava et al., 2015; Vila et al., 2016). Indeed, the rigorous sampling of the Upper Cretaceous continental deposits of the Ibero-Armorican domain has led to the discovery of around 500 Campanian to Maastrichtian dinosaur-bearing sites (Vila et al., 2016). The Ibero-Armorican dinosaur sites from the uppermost Cretaceous are mainly distributed across the regions of Occitania, Provence, and the Southern Pyrenees (southern France and northern Spain), and the Iberian basins (Portugal and Spain) (Vila et al., 2016; Fondevilla et al., 2019; Aurell et al., 2022). The study of this dinosaur record has revealed a faunal turnover that affected dinosaur communities during the Maastrichtian (Le Loeuff et al., 1994; Sellés et al., 2014; Vila et al., 2016; Fondevilla et al., 2019). This faunal change mostly involved the assemblages of herbivorous dinosaurs, differentiating a Campanian-early Maastrichtian assemblage with rhabdodontid ornithopods, nodosaurid ankylosaurians, and titanosaurian sauropods, from a late Maastrichtian assemblage dominated by hadrosaurid ornithopods and other titanosaurian sauropods. These two assemblages coexisted during an interval of around 2.5 Ma, from the beginning of chron C31r to the end of chron C30r, although the

* Corresponding author.
E-mail addresses: erik.isasmendi@ehu.eus (E. Isasmendi), manuppueyo@unizar.es (M. Pérez-Pueyo), mmazanza@unizar.es (M. Moreno-Azanza), talonsog@proton.me (A. Alonso), puertolas@unizar.es (E. Puértolas-Pascual), bbadenas@unizar.es (B. Bádenas), jicanudo@unizar.es (J.I. Canudo).

https://doi.org/10.1016/j.cretres.2024.105952

disappearance of each of the pre-turnover groups is not synchronous (Fondevilla et al., 2019). By contrast, theropod assemblages seem to have been unaffected by the turnover, with medium-sized abelisauroids, small maniraptorans, and avialans characterizing the theropod assemblage during the entire Maastrichtian. However, the theropod oological record from the Ibero-Armorican domain appears to show that theropods were also somewhat affected, since two different eggshell associations can be recognized during the Campanian–lower Maastrichtian and the upper Maastrichtian, respectively (Sellés et al., 2014). Either way, the scarce osteological record of theropod dinosaurs in Ibero-Armorica has hindered more detailed interpretations.

Among the present-day areas of the former Ibero-Armorican Island, the South Pyrenean Basin represents one of the best-known zones (Pérez-Pueyo et al., 2021a) based on detailed studies that have improved our understanding of the palaeobiodiversity of vertebrates, their palaeoenvironments, and their chronostratigraphic framework (Canudo et al., 2016; Vila et al., 2016; Fondevilla et al., 2019). Although fragmentary and isolated theropod postcranial remains are known from this area (e.g., Blanco et al., 2015; Pérez-Pueyo et al., 2019, 2021b; Isasmendi et al., 2021), some of which have led to the description of the first European jinfengopterygine troodontid *Tamarro insperatus*, most of the theropod record from the South Pyrenean Basin is represented by isolated teeth (e.g., Torices et al., 2015; Marmi et al., 2016; Sellés et al., 2021; Isasmendi et al., 2022). The appearance of new methodologies and exhaustive studies of theropod dentition (e.g., Hendrickx et al., 2015a, 2019 and references therein) has made it possible for the revision and study of the herein studied material to achieve the most accurate picture yet of the theropod fossil record in the South Pyrenean Basin.

The purpose of this paper is: 1) to revise the previously published dental specimens and analyze new isolated theropod teeth recovered from several sites from the western sector of the Tremp Syncline; 2) to perform morphometric and cladistic analyses using the studied sample; and 3) to evaluate the effects that the intra-Maastrichtian faunal turnover had on non-avian theropods, based on the identification of the new theropod dental material.

2. Geographical and geological setting

The dental material studied here was recovered from upper Maastrichtian deposits from the topmost Arén Formation (Fm) and Tremp Fm outcropping in the county of Ribagorza (Huesca Province, Aragón, NE Spain) in the Southern Pyrenees. The Pyrenees are a mountain chain situated in the northeast of the Iberian Peninsula, resulting from the collision between the Iberian and European plates during the Alpine orogeny, uplifting the range as a double-vergence belt of thrusts and folds (Teixell, 1998; Sibuet et al., 2004). The asynchronous movement of the different thrust sheets from the Late Cretaceous to the Miocene generated a set of foreland basins, some of which were stacked as piggyback basins (Muñoz, 1992; Chanvry et al., 2018; Muñoz et al., 2018). This is the case with the South Pyrenean Basin (Fig. 1A), which is compartmentalized into different synform syntectonic sub-basins bounded by thrusts (Fondevilla et al., 2016a). The Tremp Syncline (Fig. 1A) is the largest of these sub-basins. Its uppermost Cretaceous and Paleocene sedimentary record encompasses marine, transitional, and continental deposits, including (Fig. 1B): 1) the coarse bioclastic barrier-island sandstones of the Arén or Arén Sandstone Fm (middle Campanian–Maastrichtian) (Nagtegaal et al., 1983; Mutti and Sgavetti, 1987); and 2) the transitional and continental successions of the Tremp Fm (Maastrichtian–Paleocene; Mey et al., 1968), which overlies and passes laterally to the Arén Fm (Ardévol et al., 2000; Fondevilla et al., 2016a).

The Tremp Fm, traditionally known as the 'Garumnian facies' in the Pyrenees (Leymerie, 1868), includes, from base to top, four informal units (Fig. 1B; Rosell et al., 2001; Pérez-Pueyo et al., 2021a). These are the 'Grey Garumnian', the 'Lower Red Garumnian', the 'Vallcebre limestones and equivalents', and the 'Upper Red Garumnian'. The 'Grey Garumnian' is composed of grey marls and mudstones, with some intercalations of sandstones, limestones, and occasional coal beds, displaying a rich record of mixed marine and freshwater invertebrate faunas and thus indicating deposition in transitional environments such as lagoons, tidal mud flats, and marshes (Eichenseer, 1988; Rosell et al., 2001; Díez-Canseco et al., 2014; Oms et al., 2016). The 'Lower Red Garumnian' is made up of multi-colored mudstones with palaeosoils, and intercalations of lenticular sandstone packages and occasional lacustrine carbonates, interpreted as perilagoonal and fluvial deposits with a certain tidal influence (Eichenseer, 1988; Rosell et al., 2001; Riera et al., 2009; Díez-Canseco et al., 2014). The 'Grey Garumnian' and 'Lower Red Garumnian' are interfingered, the 'Grey Garumnian' passing gradually into the 'Lower Red Garumnian', and they have been dated as latest Campanian–Maastrichtian (Fig. 1B) (Díez-Canseco et al., 2014; Vicente et al., 2015, 2016; Fondevilla et al., 2016a; Puértolas-Pascual et al., 2018). The two remaining units of the Tremp Fm are Paleocene in age, the lacustrine 'Vallcebre limestones' being dated as Danian, and the fluvial 'Upper Red Garumnian', as Selandian to Thanetian (Serra-Kiel et al., 1994; Ullastre and Masriera, 1998; Rosell et al., 2001; Díez-Canseco et al., 2014).

The upper Maastrichtian theropod teeth under study come from seven sites from the topmost Arén Fm and Tremp Fm in the Western Tremp Syncline (Fig. 1). The deposits of the Arén and Tremp formations have been dated as latest Maastrichtian in this area, ranging from the top of magnetochron C30n to chron C29r, which corresponds to the last 300 kyr of the Cretaceous before the K/Pg boundary (López-Martínez et al., 2001; Pereda-Suberbiola et al., 2009; Canudo et al., 2016; Puértolas-Pascual et al., 2018). From base to top, the stratigraphic locations of the sites are: the Blasi 1 locality (1 in Fig. 1B) (Arén/Areny, Arén municipality), located in the topmost part of the Arén Fm, in the 'Grey Garumnian', Blasi 2B (2 in Fig. 1B) and Blasi 3 (3 in Fig. 1B) (Arén/Areny, Arén municipality); Veracruz 1 (4 in Fig. 1B) (Biascas de Obarra, Beranuy municipality) and 172-i/04/e (5 in Fig. 1B) (Serraduy, Isábena municipality); and finally two sites located in the 'Lower Red Garumnian', Larra 4 (7 in Fig. 1B) ((Sala, Valle de Lierp municipality) and Amor 3 (8 in Fig. 1B) (Beranuy, Beranuy municipality)). In the 'Lower Red Garumnian', an additional locality has provided theropod fossils: Dolor 2/3 (6 in Fig. 1B), where a vertebra from a large ornithuromorph avialan was found (Pérez-Pueyo et al., 2021b).

3. Methodology

3.1. Studied material

A total of 31 isolated teeth from the seven sites were studied. The teeth were recovered between 1998 and 2021 via surface prospection during excavation campaigns or by screen-washing of sediments by members of the Aragosaurus-IUCA research group of the Universidad de Zaragoza. The material is curated at the Museo de Ciencias Naturales de la Universidad de Zaragoza, Spain (Canudo, 2018). All the teeth were given their corresponding museum acronyms (MPZ) as listed hereafter: MPZ 98/67 to MPZ 98/82, MPZ 2004/3 to MPZ 2004/8, MPZ 2017/804, MPZ 2019/189, MPZ 2021/223 and MPZ 2022/80 to MPZ 2022/90. Some of these teeth were studied previously by other authors: MPZ 98/67 to MPZ 98/82 were first studied by López-Martínez et al. (2001) and were

reidentified by Torices et al. (2015), who additionally studied specimens MPZ 2004/3 to MPZ 2004/8, whereas specimens MPZ 2017/804 and MPZ 2019/189 were first described by Puértolas-Pascual et al. (2018). Specimens MPZ 2021/223 and MPZ 2022/80 to MPZ 2022/90 are studied for the first time in this paper.

The teeth were examined firsthand under stereo (Olympus SZ-STS) and Dino-Lite Edge digital (AM7915MZT) microscopes. The measurements of the larger teeth were taken with a digital caliper (Juning) whereas the smaller teeth and the denticle densities of the larger ones were measured with the ImageJ program (Rasband, 2003) using the photographs taken with the Dino-Lite on the original teeth. Small teeth were gold-coated and photographed with a JEOL JSM 6400 scanning electron microscope (SEM) housed at the 'Servicio de Microscopía Electrónica de Materiales' of the University of Zaragoza (Spain).

3.2. Comparative methodology and terminology

The dental nomenclature and methodology applied in this work are based on those proposed by Hendrickx et al. (2015a) and references therein. Both the qualitative and quantitative characters used for the study of the teeth follow those of Currie et al. (1990), Smith et al. (2005), and Hendrickx et al. (2015a). The qualitative features used to identify the teeth are the crown shape, type and cross-section, the position and extension of the carinae, if present, the presence or absence of denticles, denticle morphology and their position along the carinae, and crown ornamentation. The measurements taken on all teeth are as follows (Fig. 2): crown base length (CBL), crown base width (CBW), mid-crown length (MCL), mid-crown width (MCW), crown height (CH), and apical length (AL). Furthermore, the crown base ratio (CBR; defined as CBW/CBL) and the crown height ratio (CHR; defined as CH/CBL) were calculated for each specimen. For the larger teeth the mesioapical denticle density (MA), the mesiocentral denticle density (MC), the mesiobasal denticle density (MB), the distoapical denticle density (DA), the distocentral denticle density (DC), and the distobasal denticle density (DB) were also measured per 5 mm. These measurements could not be taken on the smaller teeth, and so only the mesiocentral denticle density (MC) and the distocentral denticle density (DC) per 1 mm were measured; these were normalized to 5 mm afterwards. Finally, the denticle size density index (DSDI; defined as MC/DC) was calculated for all the specimens. Some values were estimated for the almost complete teeth, following the outline of the tooth (see Supplementary material 1).

3.3. Discriminant analyses

Various discriminant analyses (DAs) were carried out using PAST 4.05 (Hammer et al., 2001). The database used for the analyses is mainly based on the one published by Hendrickx et al. (2015b). In addition to the specimens measured directly by Hendrickx et al. (2015b), this dataset collects morphometric information from Cope (1876), Farlow et al. (1991), Park (2000), Sankey et al. (2002, 2005), Currie and Varricchio (2004), Smith (2005), Smith et al. (2005), Smith and Lamanna (2006), Smith and Vecchia (2006), Fanti and Therrien (2007), Longrich (2008), Sankey (2008), Sereno and Brusatte (2008), Hocknull et al. (2009), Molnar et al. (2009), and Larson and Currie (2013). The teeth attributed to *Zapsalis* were removed from the database because they turned out to be premaxillary teeth of dromaeosaurids such as *Saurornitholestes* (Currie and Evans, 2020). The teeth of '*Megalosaurus dunkeri*' published by Ősi et al. (2010) and *Nuthetes* were also eliminated due to their uncertain affinities. In line with Hendrickx et al. (2020), moreover, the teeth formerly assigned to *Spinosaurus* are here regarded as Spinosaurinae indet. As well as this database, other teeth with morphometric data collected by Currie and Azuma (2006), Gianechini et al. (2011a), Evans et al. (2013), Tortosa et al. (2014), White et al. (2015), Gerke and Wings (2016), Longrich et al. (2017), Malafaia et al. (2017), Young et al. (2019), and Isasmendi et al. (2022) were also considered. With all these changes, the database used in the discriminant analyses consists of 1159 teeth and 65 taxa, including some indeterminate spinosaurid teeth, an unnamed dromaeosaurid, and an unnamed megaraptoran.

Many variables have been used in performing the morphometric analyses. However, not all the databases include all these variables. For instance, Young et al. (2019) and Hendrickx et al. (2020) used the denticle length instead of denticle densities to include mostly metric-based variables. Unfortunately, the teeth of many taxa that are interesting for this study lack these measurements. Therefore, only the previously most widely used variables (CBL, CBW, CH, CBR, CHR, MC and DC) were applied to the DAs, even though other variables were also measured on the studied teeth. Before performing the DAs, the data were normalized with Log $(x + 1)$ in order to be able to use data with zero values. Furthermore, the sample studied herein was not previously grouped for the analyses, and only the teeth from the database built for this study were grouped as they were previously assigned (65 groups in total).

In total, four discriminant analyses were performed: (1) DA1, at taxon level with five variables (CBL, CBW, CH, MC and DC); (2) DA2, at group or clade level with five variables (CBL, CBW, CH, MC and DC); (3) DA3, at taxon level with seven variables (CBL, CBW, CH, CBR, CHR, MC and DC); and (4) DA4, at group or clade level with seven variables (CBL, CBW, CH, CBR, CHR, MC and DC). Note that as the position of *Paronychodon* and *Richardoestesia* within Theropoda is still undetermined, these taxa were not included in any clade or group in DA2 and DA4, instead being considered as belonging to distinct groups.

3.4. Cladistic analyses

To analyze the phylogenetic relationships of the different tooth morphotypes, the teeth were subjected to several dental-based cladistic analyses. All the teeth were scored in the matrix used by Meso et al. (2021) (see Supplementary materials 2 and 3), which is an updated version of the original matrix created by Hendrickx and Mateus (2014). This version of the matrix presents 146 characters (16 ordered) which are scored for 105 different theropod genera plus two additional terminal taxa: a juvenile specimen of *Limusaurus* and MPC-D100-1323, a troodontid with affinities to *Almas ukhaa*. Although each of the teeth was codified for the matrix (see Supplementary material 2), to simplify the number of analyses, we considered each dental morphotype as a separate terminal taxon. The matrix uses several topological constraints on the data to obtain a backbone topology that fulfills the current phylogenetic consensus on theropod dinosaurs. This consensus is based on the results from Müller et al. (2018) for non-neotheropod Saurischia, Ezcurra (2017) for non-averostran Neotheropoda, Rauhut and Carrano (2016) and Wang et al. (2017) for Ceratosauria, Carrano et al. (2012) and Rauhut et al. (2012, 2016) for non-coelurosaurian Tetanurae, Brusatte and Carr (2016) for Tyrannosauroidea, and Cau et al. (2017) for non-tyrannosauroid Coelurosauria.

The analyses were carried out using TNT 1.5 (Goloboff and Catalano, 2016) (see Supplementary material 3 for the TNT script, which includes the search parameters that were used), following the methodology proposed by Hendrickx et al. (2020). Space for up to 50,000 trees was allocated in memory for each analysis (Enter command *Hold 50000*). For each analysis, first a New Technology search with a combination of different tree-search algorithms was conducted, using TBR branch swapping, sectorial searches, Ratchet

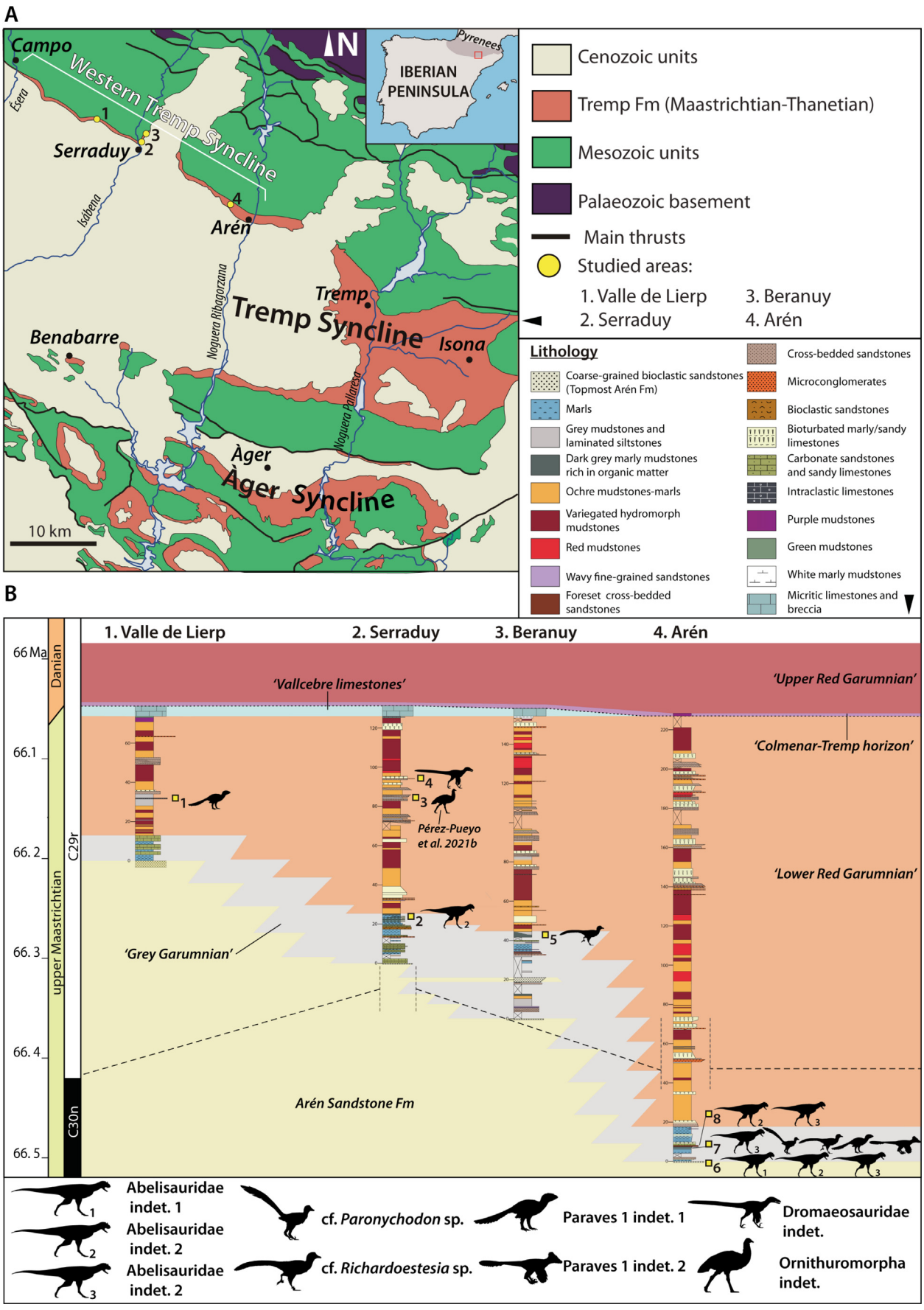
A
Campo
Western Tremp Syncline
Ésera
Serraduy
Isábena
Arén
Noguera Ribagorzana
Tremp
Tremp Syncline
Benabarre
Isona
Noguera Pallaresa
Àger
Àger Syncline
10 km
N
Pyrenees
IBERIAN PENINSULA
Cenozoic units
Tremp Fm (Maastrichtian-Thanetian)
Mesozoic units
Palaeozoic basement
Main thrusts
Studied areas:
1. Valle de Lierp
2. Serraduy
3. Beranuy
4. Arén
Lithology
Coarse-grained bioclastic sandstones (Topmost Arén Fm)
Marls
Grey mudstones and laminated siltstones
Dark grey marly mudstones rich in organic matter
Ochre mudstones-marls
Variegated hydromorph mudstones
Red mudstones
Wavy fine-grained sandstones
Foreset cross-bedded sandstones
Cross-bedded sandstones
Microconglomerates
Bioclastic sandstones
Bioturbated marly/sandy limestones
Carbonate sandstones and sandy limestones
Intraclastic limestones
Purple mudstones
Green mudstones
White marly mudstones
Micritic limestones and breccia
B
1. Valle de Lierp
2. Serraduy
3. Beranuy
4. Arén
66 Ma
66.1
66.2
66.3
66.4
66.5
Danian
upper Maastrichtian
C29r
C30n
'Vallcebre limestones'
'Upper Red Garumnian'
'Colmenar-Tremp horizon'
'Lower Red Garumnian'
'Grey Garumnian'
Arén Sandstone Fm
Pérez-Pueyo et al. 2021b
Abelisauridae indet. 1
Abelisauridae indet. 2
Abelisauridae indet. 2
cf. Paronychodon sp.
cf. Richardoestesia sp.
Paraves 1 indet. 1
Paraves 1 indet. 2
Dromaeosauridae indet.
Ornithuromorpha indet.

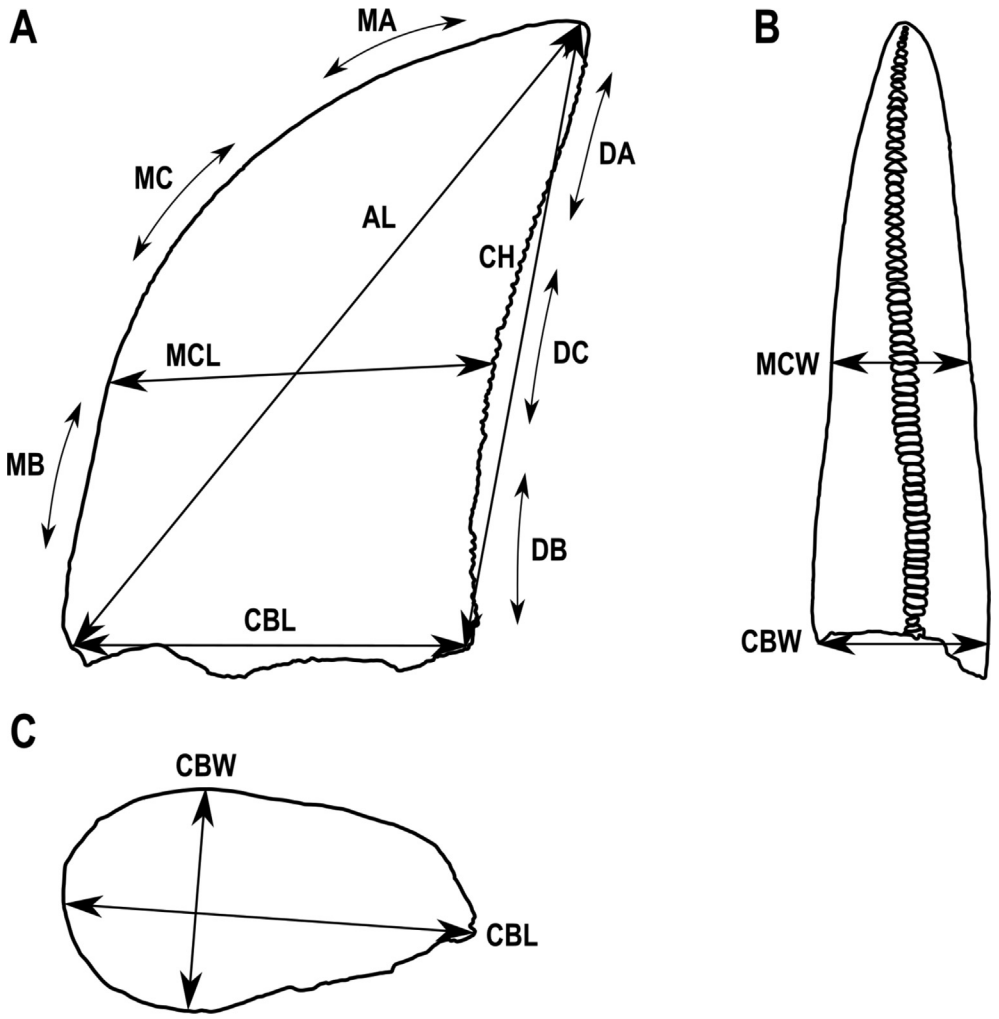

Fig. 2. Morphometric terminology used for the studied tooth specimens. A, theropod tooth in lateral view. B, theropod tooth in distal view. C, theropod tooth in basal view. Abbreviations: AL, apical length; CBL, crown base length; CBW, crown base width; CH, crown height; DA, distoapical denticle density; DB, distobasal denticle density; DC, distocentral denticle density; MA, mesioapical denticle density; MB, mesiobasal denticle density; MC, mesiocentral denticle density; MCL, mid-crown length; MCW, mid-crown width (based on Hendrickx et al., 2015a).

(stopping the perturbation phase after 20 substitutions) and Tree Fusing (5 rounds), until 100 hits of the same minimum tree length were reached (Enter command *xmult = hits 100 rss fuse 5 ratchet 20*). After that, the trees obtained were subjected to an additional round of TBR branch swapping (Enter command *bb*). A first round of analysis was carried out using a constrained topology (Enter command *constrain=*) with all eight morphotypes acting as floating taxa. As it was difficult to determine whether the teeth assigned to cf. *Paronychodon* sp. and cf. *Richardoestesia* sp. belong to mesial or to lateral teeth, this initial analysis was run twice, scoring these two morphotypes in one case as mesial teeth, and in the other as lateral teeth. A second round of constrained analyses was performed, using each of the eight morphotypes separately, running twice for cf. *Paronychodon* sp. and cf. *Richardoestesia* sp. (mesial and lateral). Finally, two more analyses were conducted, deactivating the constraints (Enter command *constrain-*) and using the 8 OTUs altogether (again repeating one analysis for the mesial and another for the lateral scores of cf. *Paronychodon* sp. and cf. *Richardoestesia* sp.) In total 14 different analyses were carried out.

Institutional abbreviations: IIPG, Instituto de Investigación en Paleobiología y Geología, General Roca, Río Negro, Argentina; MNHN, Muséum National d'Histoire Naturelle, Paris, Paris, France; MPZ, Museo de Ciencias Naturales de la Universidad de Zaragoza, Zaragoza, Aragón, Spain; UPUAM, Unidad de Paleontología, Universidad Autónoma de Madrid, Madrid, Spain.

4. Systematic palaeontology

DINOSAURIA Owen, 1842
THEROPODA Marsh, 1881
CERATOSAURIA Marsh, 1884
ABELISAURIDAE Bonaparte and Novas, 1985

Remarks. Three dental morphotypes (1, 2 and 3) have been referred to Abelisauridae.

Abelisauridae indet. 1

Material. One tooth (MPZ 2004/4 from Blasi 1; Fig. 3A–F).

Fig. 1. Geographic and geological setting of the uppermost Cretaceous fossil sites with theropod remains from the Western Tremp Syncline. A, Geological map of the western sector of the South Pyrenean Basin, with emphasis on the Tremp Syncline and the location of the fossil sites studied in this paper (modified after López-Martínez and Vicens, 2012). B, Time-calibrated NW-SE correlation panel of the Western Tremp Syncline, with the stratigraphic position of the theropod fossil-bearing sites: 1) Blasi 1; 2) Blasi 2B; 3) Blasi 3; 4) Veracruz 1; 5) 172-i/04/e; 6) Dolor 2/3; 7) Larra 4; 8) Amor 3 (modified after Pérez-Pueyo et al., 2021a). Silhouettes after Mette Aumala, Tasman Dixon, Rebecca Groom, Scott Hartman, and Emily Willoughby. For license attribution of the silhouettes, see Supplementary material 6.

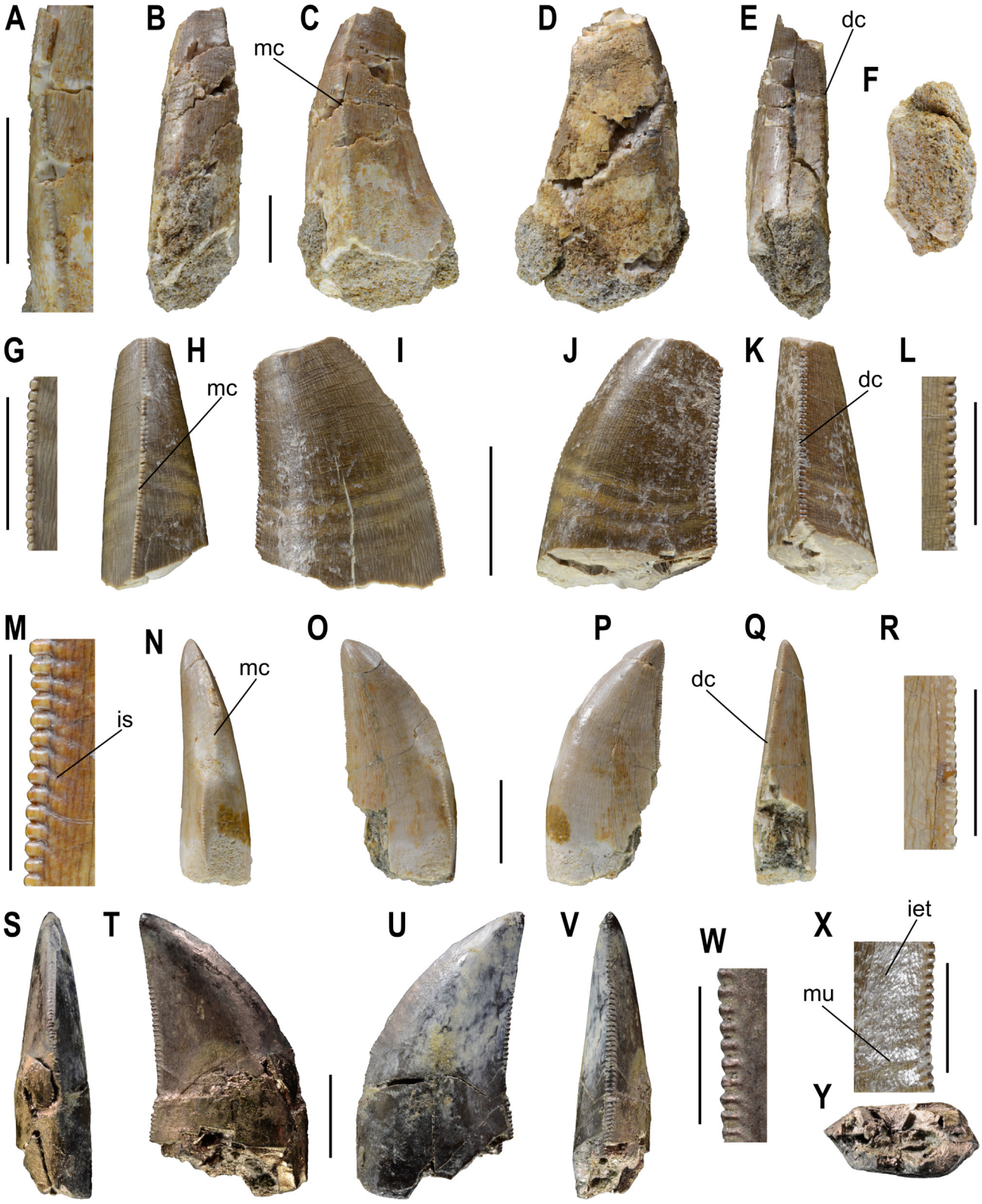

Fig. 3. Abelisauridae indet. teeth. A–F, Abelisauridae indet. 1 morphotype. A–F, MPZ 2004/4, mesial carina, crown in mesial, lingual, labial and distal views, basal cross-section. G–M and X, Abelisauridae indet. 2 morphotype. G–L and X, MPZ 2017/804, mesial carina and mesial denticle close-up, crown in mesial, lingual, labial and distal views, and distal carina, distal denticle close-up, and enamel texture. M, MPZ 2021/223, close-up of distal carina and denticles. N–Y, Abelisauridae indet. 3 morphotype. N–R, MPZ 2022/81 crown in mesial, lingual, labial and distal views, and distal denticle close-up. S–W and Y, MPZ 2004/6 crown in mesial, lingual, labial and distal views, distal denticle close-up, and basal cross-section. Scale bars equal 1 cm, except for denticles and textures (0.5 cm). Abbreviations: mc, mesial carina; dc, distal carina; iet, irregular enamel texture; is, interdenticular sulcus; and mu, marginal undulation.

Description. Specimen MPZ 2004/4 lacks the apex and parts of the enamel, especially on the labial margin and the carinae. Some horizontal and vertical fractures are also present. Most of the denticles are eroded, but their bases are still preserved.

The crown is ziphodont, but not especially labiolingually compressed apically, and quite elongated. It seems that the crown would be distally curved if the apex was present, but the apex would not extend beyond its basodistalmost point (Fig. 3C and D). In lateral views, the distal margin is slightly concave, whereas the mesial margin is convex (Fig. 3C and D). Both labial and lingual surfaces are mesiodistally convex, with the convexity being more prominent on the lingual surface in distal or mesial views (Fig. 3B and E). The labial surface is apicobasally virtually flat, but the lingual surface is more concave (Fig. 3B and E). The lingual surface has concave surfaces adjacent to the mesial and distal carinae. The concavity near the mesial carina is more marked than the one near the distal carina. These concavities are more pronounced and wider basally (Fig. 3A–E). The basal cross-section of the crown is J-shaped (Fig. 3F), and the mid-crown cross-section is between salinon- and parlinon-shaped (*sensu* Hendrickx et al., 2015a). No basal constriction is present in the tooth.

The CBL measures 22.93 mm whereas the CBW is 12.38 mm, with a CBR of 0.54. Apically, the length of the crown decreases proportionally more than the width, making the tooth appear less compressed.

Both mesial and distal carinae are present and denticulated, and seem to have reached the cervix or would have at least extended close to it (Fig. 3A, C and E). The mesial carina is diagonally oriented and lingually displaced, especially basally (Fig. 3C). By contrast, the distal carina is strongly labially displaced and straighter and follows the curvature of the crown (Fig. 3E). On average, the mesial denticles are slightly smaller than the distal ones, with around 12.05 and 11.66 denticles per 5 mm, respectively. The denticles become gradually smaller towards the cervix. There is no random variation in denticle size along the carinae. Interdenticular sulci are present along both carinae. These are subtle, short, and basally inclined.

Some subtle transverse undulations are present on the enamel. The enamel exhibits micro-scratches and is polished. The enamel texture is subtle, non-oriented, and irregular (*sensu* Hendrickx et al., 2015a).

Abelisauridae indet. 2

Material. Four teeth (MPZ 2017/804 from 172-i/04/e; and MPZ 2021/223, MPZ 2022/87, and MPZ 2022/88 from Blasi 3; Fig. 3G–M and X).

Description. None of the teeth is complete, but MPZ 2022/88 is nearly complete, and the denticles are particularly well preserved in MPZ 2017/804. The crowns are ziphodont, labiolingually compressed, and slightly distally curved (Fig. 3G–L). The distal extension of the apex with respect to the basal length cannot be determined in most of the crowns, but in MPZ 2022/87 the apex seems not to have extended beyond the basodistalmost point of the crown. The mesial margin of these teeth is always convex, whereas the distal margin is straight in MPZ 2017/804 (Fig. 3I and J) and MPZ 2021/223, and gently concave in MPZ 2022/87 and MPZ 2022/88. In mesial or lingual view, both labial and lingual surfaces are convex in most of the crowns, especially the labial surfaces (Fig. 3H and K). However, this cannot be clearly assessed in MPZ 2022/87 due to its poor state of preservation. The lingual and labial surfaces are convex in all the teeth, but MPZ 2017/804 exhibits a concave surface adjacent to the distal carina on the lingual surface (Fig. 3I). This concave surface is more pronounced basally and fades apically. In MPZ 2021/223, this surface is planar instead of concave. The basal cross-section is lanceolate in MPZ 2021/223, and the mid-crown cross-section is lenticular in all the specimens. In MPZ 2021/223, this cannot be evaluated, but it is not basally constricted.

The CBL varies between 9.81 and 17.74 mm, whereas the CBW ranges from 6.85 to 11.71 mm, giving a CBR between 0.65 and 0.69. In other words, the basal width is more than half of the basal length. The CH varies between 14.57 and 30.14 mm, and the AL ranges from 17.56 to 32.63 mm, indicating that the crowns are not very distally curved. The CHR varies between 1.24 and 2.85.

All the teeth have denticulated mesial and distal carinae, when preserved (Fig. 3G and L). In MPZ 2022/88, the mesial carina is diagonally oriented and reaches the cervix. In MPZ 2017/804, it would most likely extend from the apex to further basally than mid-crown. The mesial carina of MPZ 2017/804 is apically centered and is gradually displaced strongly lingually (Fig. 3H), and in MPZ 2022/88 it remains virtually centered along its entire extension but is slightly displaced lingually near the cervix. The distal carina reaches the cervix in MPZ 2021/223. This is slightly bowed and labially displaced (Fig. 3K).

The denticles are largest at mid-crown and get slightly smaller apically and especially basally (Fig. 3H and K). There is no random variation in denticle size along the carinae. The denticles are almost equal in size or slightly larger on the mesial carina, with DSDI values ranging from 0.86 to 1.083. The mesial denticle density varies between 13 and 14 denticles per 5 mm, and the distal denticle density ranges from 10 to 14 denticles per 5 mm. The denticles are symmetrical or slightly symmetrically convex in outline and perpendicular to the carinae, but they are slightly apically inclined in MPZ 2021/223. The mesial denticles are subquadrangular or slightly apicobasally subrectangular (Fig. 3G), whereas the distal denticles are subquadrangular or mediodistally subrectangular (Fig. 3L). In MPZ 2017/804, interdenticular sulci are present on both labial and lingual surfaces of the mesial and distal carinae. In MPZ 2021/223, these are present and especially pronounced between its distal denticles (Fig. 3M). The interdenticular sulci are subtle, short, straight, and basally inclined.

Transverse undulations are present on the enamel of MPZ 2017/804 and MPZ 2021/223. Furthermore, MPZ 2017/804 exhibits marginal undulations on both mesial and distal carinae. These are especially abundant on the distal carina. In the specimens that are not polished, the enamel texture is non-oriented and irregular (*sensu* Hendrickx et al., 2015a) (Fig. 3X).

Abelisauridae indet. 3

Material. Eight teeth (MPZ 2004/3 and MPZ 2022/81 from Blasi 1; MPZ 2004/5 and MPZ 2004/6 from Blasi 2B; and MPZ 98/67, MPZ 2004/8, MPZ 2022/86, and MPZ 2022/89 from Blasi 3; Fig. 3N–W and Y).

Description. Most of the teeth are not complete. The only complete crown is MPZ 2004/6, whereas MPZ 2004/8, MPZ 2022/81, and MPZ 2022/89 are nearly complete.

The crowns are ziphodont, labiolingually compressed, and with apices that are distally curved. However, these seem not to extend beyond the basodistalmost point of the crown in MPZ 2004/8 and MPZ 2022/81, although it appears to do so in MPZ 2004/6 (Fig. 3O, P, T and U). The mesial margins of all the specimens, if preserved, are convex, whereas the distal profiles vary depending on the crown. The distal margins are straight or nearly straight in MPZ 98/67 and MPZ 2022/81, whereas they are gently concave in MPZ 2004/6, MPZ 2004/8 and MPZ 2022/89 (Fig. 3O, P, T and U). In mesial or lingual view, both the labial and especially the lingual surfaces are convex in most of the crowns. MPZ 2022/81 exhibits a slightly concave lingual margin that becomes convex apically in distal view (Fig. 3O). The lingual and labial surfaces are convex, but concave surfaces adjacent to the distal carinae can be noticed on the lingual area in MPZ 2004/8 and MPZ 2022/86. These concave areas are more

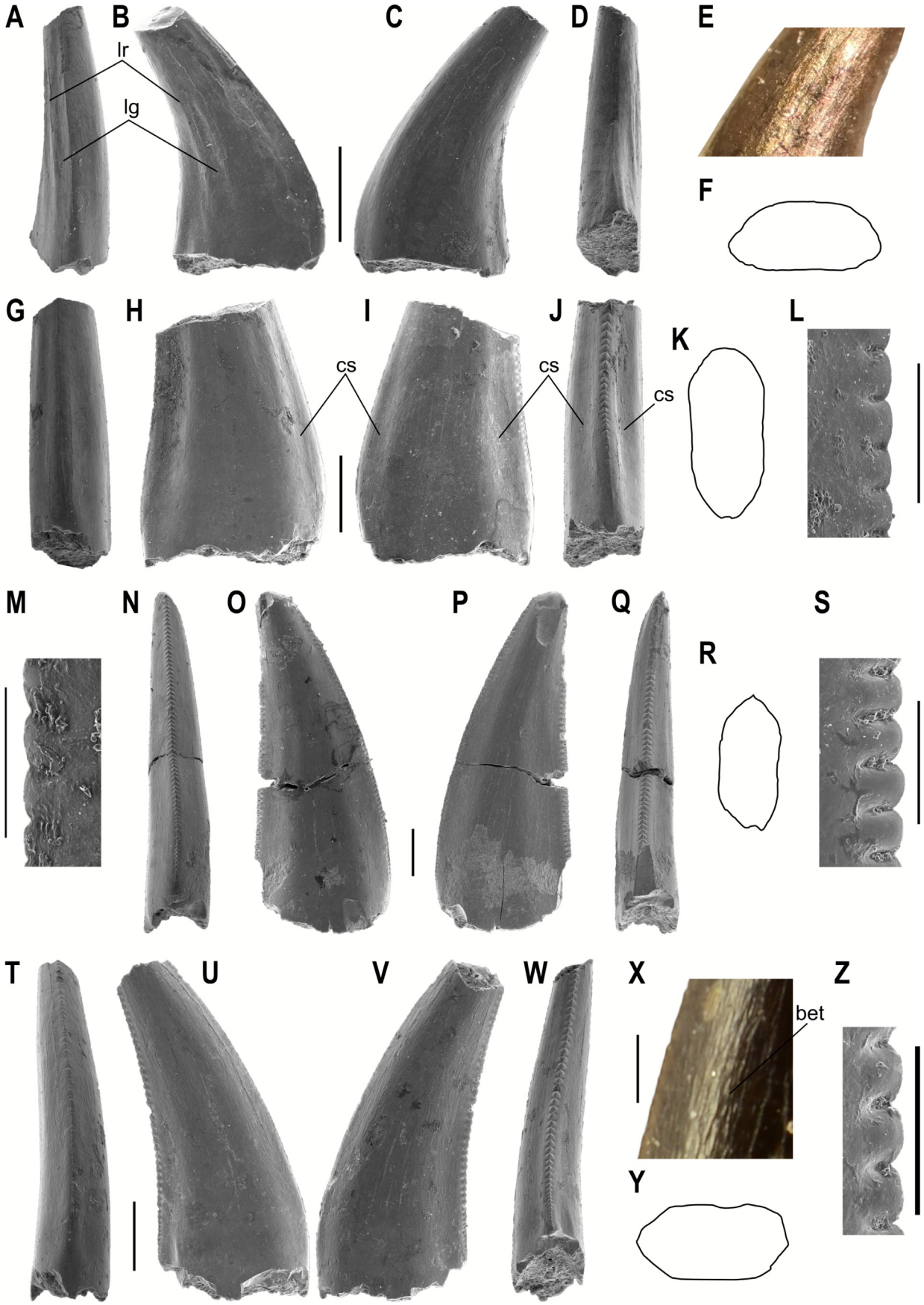
A
B
lr
lg
C
D
E
F
G
H
cs
I
cs
J
cs
K
L
M
N
O
P
Q
R
S
T
U
V
W
X
bet
Y
Z

pronounced basally and fade apically. The basal cross-sections of the crowns vary between figure-eight-shaped (MPZ 2004/8), lanceolate (MPZ 2004/6, MPZ 2022/81 and MPZ 2022/89, although in MPZ 2022/81 a basally located and centrally positioned depression on the labial side makes it almost reniform) (Fig. 3Y), oval (MPZ 98/67), and reniform (MPZ 2022/86). The mid-crown cross-sections of the most complete crowns are lenticular, although this feature cannot be evaluated in MPZ 2004/3 and MPZ 2004/5 due to their incompleteness. There are no noticeable basal constrictions in any specimens.

The CBL ranges from 6.57 to 20.97 mm, whereas the CBW varies between 3.77 and 12.91 mm, and the CBR between 0.5 and 0.61. In other words, the basal width is half or slightly more than half the basal length. The CH ranges from 12.3 to 28.91 mm, and the AL from 13.7 to 30.87 mm. The values for CH and AL match closely in all these teeth, but MPZ 2022/89 and MPZ 2004/6 indicate that the crowns are not very distally curved. The CHR varies between 1.57 and 2.28.

All the crowns exhibit denticulated mesial and distal carinae, when preserved (Fig. 3N–W). The mesial carinae are diagonally oriented and reach the cervix or extend slightly beyond it in MPZ 2004/6 and MPZ 2022/81 (Fig. 3N). Although this cannot be assessed with certainty, it seems that in MPZ 98/67, MPZ 2004/5, MPZ 2004/8, and MPZ 2022/89 the mesial carina would have extended further basally than mid-height starting from the apex. The mesial carinae are centered apically and are gradually but quite strongly displaced lingually in MPZ 2004/6 (Fig. 3S), MPZ 2004/8, MPZ 2022/81 (Fig. 3N), and MPZ 2022/89. MPZ 2022/81 has an abnormal mesial carina. Below a possible lesion located at mid-crown, the mesial carina drastically curves lingually (Fig. 3N). The distal carinae also reach the cervix in all the specimens that preserve them (Fig. 3V). These are labially displaced in all the specimens except in MPZ 2004/6 and MPZ 2022/81. In MPZ 2022/81, the distal carina is somewhat twisted, being apically centered and labially displaced basally (Fig. 3N). In MPZ 2004/6, it is almost centered, but still slightly labially displaced basally (Fig. 3V).

The denticles are larger near the middle of the carinae and gradually become smaller especially towards the cervices and slightly so towards the apices. The denticles do not change randomly in size along the carinae (Fig. 3R and W). The mesial denticles are also smaller or almost equal in size on the mesial carinae compared to the distal denticles, with DSDI values varying between 1.02 and 1.125. The average mesial denticle densities range from 13.5 to 19 denticles per 5 mm, whereas the average distal denticle densities vary from 12.6 to 17.08 denticles per 5 mm. The denticles are not apically hooked. Indeed, the outline of the denticles is symmetrical or slightly asymmetrically convex (Fig. 3R and W). These are perpendicular to the carinae in most of the crowns but are slightly apically inclined near the apex in MPZ 2022/81. The mesial denticles are subquadrangular or slightly apicobasally subrectangular, whereas the distal denticles are subquadrangular or mediodistally subrectangular (Fig. 3R and W). Interdenticular sulci are present in both labial and lingual surfaces of the mesial and distal carinae on the better-preserved specimens (MPZ 2004/6 and MPZ 2022/81) and between the distal denticles of MPZ 2004/8 and MPZ 2022/86 (Fig. 3W). These always occur along the carinae. Overall, the interdenticular sulci are subtle, short, straight, and basally inclined. Transverse undulations are present on the enamel of MPZ 98/67, MPZ 2004/3, MPZ 2004/8, MPZ 2022/81 and MPZ 2022/86. Furthermore, marginal undulations are also present on the mesial carina of MPZ 2004/6. The enamel is polished in many specimens, and micro-scratches are also present. However, the enamel textures of the teeth are non-oriented and irregular (*sensu* Hendrickx et al., 2015a).

TETANURAE Gauthier, 1986
COELUROSAURIA Marsh, 1884
FAMILY INDET.
PARONYCHODON Cope, 1876
Cf. *Paronychodon* sp.

Material. One tooth (MPZ 98/76 from Blasi 2B; Fig. 4A–F).

Description. The tooth is composed of a virtually complete crown that is only missing its most apical part. The tooth is ziphodont, elongated and distally curved. Its apex extends beyond the basodistalmost point of the crown (Fig. 4C). Its distal profile is strongly concave, and its mesial margin is convex in lateral views (Fig. 4B and C). The labial and lingual surfaces are also convex, becoming almost flat basally in mesial or distal views (Fig. 4A and D). The lingual surface is flat whereas the labial one is convex. The basal cross-section of the tooth is reniform due to the flat lingual surface (Fig. 4F). At mid-crown, its cross-section seems to be lenticular.

The tooth is minute, with an estimated CH value of 2.69 mm and an AL value of 3.3 mm. Its CBL is 1.31 mm, and the CBW is 0.59 mm. The tooth is relatively labiolingually compressed, with a CBR of 0.45, and moderately elongated, with a CHR value of 2.05.

This specimen has both mesial and distal carinae (Fig. 4A–D). These run from the apex and extend to the cervix. The mesial carina is strongly lingually displaced and straight (Fig. 4A). The distal carina is better preserved basally and is virtually centered (Fig. 4D). None of the carinae has denticles.

The ornamentation of the tooth consists of apicobasally oriented grooves bounded by three longitudinal ridges (Fig. 4A and B). These are only present on the lingual surface of the tooth. There are 3 grooves in total, of which the middle one extends the furthest apically. The grooves do not reach the apex but follow the curvature of the tooth. The enamel texture of the tooth seems to be braided (Fig. 4E) (*sensu* Hendrickx et al., 2015a).

FAMILY INDET.
RICHARDOESTESIA Currie, Rigby and Sloan, 1990
Cf. *Richardoestesia* sp.

Material. Eight teeth (MPZ 98/72, MPZ 98/73, MPZ 98/74, MPZ 98/75, MPZ 2004/7, MPZ 2022/82 and MPZ 2022/83 from Blasi 2B; and MPZ 2022/90 from Veracruz 1; Fig. 4G–Z).

Description. Specimens MPZ 98/75, MPZ 2022/90 and MPZ 2022/82 are complete, but MPZ 98/72, MPZ 98/74 and MPZ 2004/7 are fragmentary and only preserve part of the crown. MPZ 98/73 only lacks the basal-distal part of the crown, and MPZ 2022/83 is a poorly preserved crown fragment.

The crowns are ziphodont, labiolingually compressed, relatively elongated and quite straight (Fig. 4G–Z). Their apices are distally curved, but they do not extend beyond their basodistalmost point or barely do so (Fig. 4H, I, O, P, U and V). In MPZ 98/74 and MPZ 2022/82 the apices are also slightly tilted lingually (Fig. 4T and W). The mesial profiles of the teeth are convex, whereas the distal profiles are either concave (MPZ 98/72, MPZ 2022/82 and MPZ 2022/90), relatively straight (MPZ 98/73, MPZ 98/74, MPZ 98/75, MPZ 2022/83), or convex (MPZ 2004/7) (Fig. 4H, I, O, P, U and V).

Fig. 4. Theropod teeth. A–F, cf. *Paronychodon* sp. morphotype. A–F, MPZ 98/76 in mesial, lingual, labial and distal views, enamel texture and basal cross-section scheme. G–Z, cf. *Richardoestesia* sp. morphotype. G–L, MPZ 98/72 in mesial, lingual, labial and distal views, basal cross-section scheme and distal denticle close-up. M–S, MPZ 2022/90 mesial denticle close-up, mesial, lingual, labial and distal views, basal cross-section scheme and distal denticle close-up. T–Z, MPZ 2022/82 in mesial, lingual, labial and distal views, enamel texture, basal cross-section scheme and distal denticle close-up. Scale bars equal 1 mm, except for denticles and textures (0.3 mm). Abbreviations: bet, braided enamel texture; cs, concave surface; lg, longitudinal groove; lr, longitudinal ridge.

Both labial and lingual surfaces are convex in mesial or distal views and become more straight basally (Fig. 4G, J, N, Q, U and W). These surfaces exhibit centrally located planar areas. On the lingual surfaces of MPZ 98/72, MPZ 2022/82 and MPZ 2022/90 as well as on both sides of MPZ 98/73 and MPZ 98/74, an apicobasally oriented groove is present. These grooves do not reach the apex. The basal cross-sections of the crowns are either reniform (MPZ 98/75, MPZ 2022/82 and MPZ 2022/90), oval (MPZ 98/72), or somewhat figure-eight-shaped (MPZ 98/73) (Fig. 4K, R and Y). Among the teeth of this morphotype, at least MPZ 98/72, MPZ 98/74, MPZ 98/75, MPZ 2022/82 and MPZ 2022/90 have concave surfaces adjacent to the mesial and distal carinae (Fig. 4H, I, O, P, U and V).

These specimens are small. Their CBL varies between 1.37 and 2.61 mm, whereas the CBW varies between 0.79 and 1.24 mm, with CBR values between 0.37 and 0.57. The teeth have a CH that varies between 2.78 and 6.4 mm and AL values ranging from 3.1 to 6.8 mm. The teeth range from normal in length to elongate (CHR = 1.76–2.45).

The carinae are apicobasally oriented. The distal carinae always run from the apex to the cervix. They are either straight and centered as in MPZ 98/72, MPZ 98/73, MPZ 98/74, MPZ 2004/7, MPZ 2022/83 and MPZ 2022/90 (Fig. 4J and Q), or slightly labially displaced as in MPZ 98/75. The distal carina of MPZ 2022/82 seems to be twisted, being centrally placed apically but labially displaced near the cervix (Fig. 4W). The mesial carinae do not reach the cervix but nearly do so (Fig. 4G, N and T). These can be straight and lingually displaced (MPZ 2022/82), or straight and centered (MPZ 98/72, MPZ 98/73, MPZ 98/74, MPZ 98/75, MPZ 2004/7 and MPZ 2022/90). The distal carinae are denticulated in all specimens, but the mesial carinae can either bear denticles (MPZ 98/73, MPZ 2004/7, MPZ 2022/82 and MPZ 2022/90) or not (MPZ 98/72, MPZ 98/74, MPZ 98/75). The denticles are perpendicular to the carinae. The denticles are similar in size at the apex and mid-crown, and become smaller in size basally. The denticles do not change randomly in size along the carinae, except in MPZ 2004/7, MPZ 2022/82 and MPZ 2022/90, where the mesial denticles are not as well developed. The distal denticles are proximodistally subrectangular (Fig. 4L, S and Z), whereas the mesial denticles are more subquadrangular or apicobasally subrectangular (Fig. 4M). Their outline is symmetrical to slightly asymmetrically convex. There are no apparent interdenticular sulci. The denticle density ranges from 60 to 80 denticles per 5 mm on the mesial carinae, whereas it varies from 40 to 65 denticles per 5 mm on the distal carinae, with the DSDI ranging from 1.11 to 1.33 in the crowns that have mesial denticles.

Apart from the previously mentioned apicobasally oriented grooves present on some of the crowns, the teeth do not have any ornamentation. The enamel texture seems to be braided (*sensu* Hendrickx et al., 2015a) on the crowns with better-preserved enamel (Fig. 4X).

MANIRAPTORA Gauthier, 1986
PENNARAPTORA Foth, Tischlinger and Rauhut, 2014
PARAVES Sereno, 1997
Paraves indet.

Remarks. Two Paraves indet. morphotypes (1 and 2) have been distinguished.

Paraves indet. 1

Material. Six teeth (MPZ 98/77, MPZ 98/78, MPZ 98/79, MPZ 98/80 and MPZ 98/81 from Blasi 2B; and MPZ 2019/189 from Larra 4; Fig. 5A–K).

Description. The crowns of MPZ 98/77, MPZ 98/78 and MPZ 2019/189 are complete or nearly so, whereas MPZ 98/79, MPZ 98/80 and MPZ 98/81 lack the apical part of the crown. The teeth are ziphodont, specimen MPZ 98/78 being almost conidont (CBR > 0.64), and labiolingually compressed (Fig. 5A–K). The teeth are distally curved, with their apices extending beyond their basodistalmost point, at least in the crowns that preserve their apicalmost part. Although the enamel is not well preserved on all the specimens or is polished, it seems to be braided (Fig. 5E) (*sensu* Hendrickx et al., 2015a). The teeth do not have any ornamentation or a basal constriction.

In labial or lingual views, the mesial margins are convex whereas the distal profiles are concave (Fig. 5B, C, H and I). In distal view, both labial and lingual surfaces are convex, especially the labial one, but both surfaces become straighter basally (Fig. 5D and J). Indeed, a triangular planar area can be noticed near the base of the crowns, centrally positioned on the labial and lingual surfaces. These are slight concavities in MPZ 98/77, MPZ 98/78 and MPZ 98/79 (Fig. 5B and C). The cross-section of the crowns near the base varies between lanceolate (MPZ 98/79 and MPZ 98/81), figure-eight-shaped (MPZ 98/77), elliptical (MPZ 98/78), and oval (MPZ 98/80 and MPZ 2019/189) (Fig. 5F and K). Specimens MPZ 98/77, MPZ 98/79 and MPZ 98/81 exhibit concave surfaces adjacent to the distal and mesial carinae (Fig. 5B, C and H).

This morphotype consists of small-sized teeth. The CBL ranges from 1.14 to 2.89 mm, whereas the CBW varies between 0.59 and 1.34 mm, with the CBR varying between 0.45 and 0.73. The CH ranges from 2.6 to 5 mm, and the AL from 3.25 to 5.94 mm. The CHR values are highly variable, with a minimum value of 1.73 and a maximum of 1.97.

The teeth belonging to this morphotype have both mesial and distal carinae, if preserved (Fig. 5A, D, G and J). The distal carinae reach the cervix, whereas the mesial carinae do not quite reach it in most specimens, although the crown of MPZ 98/81 bears a mesial carina that reaches the cervix (Fig. 5G). The mesial carinae are straight and lingually displaced in MPZ 98/78 and MPZ 98/80, but they are straight and centered in MPZ 98/77, MPZ 98/79 and MPZ 98/81 (Fig. 5A and G). The distal carinae are more pronounced basally. They are straight and centered in all the specimens (Fig. 5D and J). Specimen MPZ 2019/189 lacks enamel, and the carinae are not well preserved, but the distal carina seems to be straight and centered; however, the position and extension of its mesial carina cannot be assessed with certainty. There are no traces of denticles or of crenulations on the carinae.

Paraves indet. 2

Material. Two teeth (MPZ 98/82 and MPZ 2022/84 from Blasi 2B; Fig. 5L–P).

Description. Neither of the teeth is complete. Specimen MPZ 2022/84 lacks the apical portion of the crown, and MPZ 98/82 does not preserve the base of the crown, either. The teeth are ziphodont, labiolingually compressed, and lower compared to those of Paraves indet. 1. The teeth are distally recurved, with their apices extending beyond their basodistalmost point (Fig. 5M and N). Despite the apex not being preserved in MPZ 2022/84, its apicalmost preserved point already extends further distally than the base. The enamel texture is not well marked but seems to be braided (*sensu* Hendrickx et al., 2015a). The teeth are devoid of other ornamentation and do not have a basal constriction. The mesial margin is convex, and the distal profile is concave in labial or lingual views (Fig. 5M and N). In distal view, both labial and lingual surfaces are convex, especially the labial one (Fig. 5O).

In MPZ 98/82, these faces become basally straighter (Fig. 5O). The basal cross-section is reniform in MPZ 98/82 (Fig. 5P). These teeth are small in size. Their CBL varies between 1.22 and 1.32 mm, whereas the CBW ranges from 0.72 to 0.74 mm. The CH value of MPZ 98/82 is 1.8 mm, and it has a CHR value of 1.48.

The two teeth belonging to this morphotype have both mesial and distal carinae (Fig. 5L and O). The distal carinae run from the apex to

the cervix and are more pronounced basally, straight and centered. The mesial carinae almost reach the cervix. This is straight and lingually deflected in MPZ 98/82, whereas it is more centered in MPZ 2022/84.

DROMAEOSAURIDAE Matthew and Brown, 1922

Dromaeosauridae indet.

Material. One tooth (MPZ 2022/80 from Amor 3; Fig. 5Q–X).
Description. The tooth lacks its apicalmost part, and some distal denticles are broken. The tooth is labiolingually compressed, ziphodont and distally curved (Fig. 5Q–X). Its apex would have extended beyond its basodistalmost point, and it is slightly tilted lingually (Fig. 5S and T). The mesial margin is convex, whereas the distal one is concave in labial or lingual views (Fig. 5S and T). In distal or mesial views, both labial and lingual surfaces are convex, becoming straighter basally (Fig. 5R and U). The lingual surface becomes flatter or more planar distally (Fig. 5S and T). There is also a triangular planar area centrally located on the lingual surface near the base of the crown. The basal cross-section of the crown is figure-eight-shaped (Fig. 5X). The enamel texture seems to be braided (*sensu* Hendrickx et al., 2015a), but the state of preservation of the enamel does not allow an accurate identification of the texture (Fig. 5V). There are some transverse undulations, at least on the labial surface of the crown. These are horizontal and not very marked.
MPZ 2022/80 is a small crown. Its CBL measures 3.21 mm and its CBW is 1.29 mm in length, with a CBR of 0.4, indicating that the tooth is very compressed labiolingually. The measured CH is 4.72 mm, whereas the AL is 6.71 mm. The CHR is 1.47, and hence the crown is not very elongated.
The carinae are apicobasally oriented and denticulated (Fig. 5Q, R, S, T, U and W). The distal carina reaches the cervix, but the mesial carina does not (Fig. 5R and U). The mesial carina is straight and slightly lingually displaced, whereas the distal carina is more centrally positioned (Fig. 5R and U). Denticles are present along the entire preserved distal carina, but on the mesial carina these become gradually smaller and are not as well developed basally. On the distal carina the denticles gradually become smaller apically and distally. The denticles are chisel-shaped in morphology (Fig. 5Q and W). Furthermore, they are proximodistally subrectangular on the distal carina but become more subquadrangular apically. The mesial denticles are subquadrangular or slightly apicobasally subrectangular. The denticles are perpendicular to the carinae and symmetrically to asymmetrically convex in outline (Fig. 5Q and W). There is no arbitrary size variation between adjacent denticles. There are no interdenticular sulci. The denticle density varies from one carina to the other, and along the same carina. The distal denticle density at mid-crown is 30 denticles per 5 mm, whereas the denticle density on the mesial carina is 50 denticles per 5 mm. The DSDI value is 1.67.

5. Results

5.1. Discriminant analyses

In all the analyses (Fig. 6 and Supplementary material 1), Axis 1 shows most of the variance among the teeth, explaining around 70% of it, whereas the variance of Axis 2 ranges from 15% to less than 22% (Table 1). The discriminant analyses do not show high reclassification rates, with a reclassification rate of around 50% in all of them. Nevertheless, this parameter is slightly greater in DA2 and DA4, where the taxa were grouped at clade-level, and especially in DA4, where as well as grouping the taxa at clade-level, seven variables were considered (Table 1 and Supplementary material 1).

The consistency of the placement of the teeth in the discriminant analyses varies among the tooth sample (Table 2). In at least one of the discriminant analyses, but in most cases two or more, the teeth MPZ 98/67, 2004/3–2004/6, 2004/8, 2017/804, 2021/223, 2022/81, 2022/86 and 2022/88, which are among the largest in the sample, are classified as belonging to abelisaurid theropods (Table 2). With regard to the other two largest teeth, MPZ 2022/87 is classified as an allosaurid or dromaeosaurid tooth, whereas MPZ 2022/89 is assigned to *Deinonychus* or Tyrannosauroidea. Within the smallest sample, the teeth with no denticles (see Systematic palaeontology section), MPZ 98/76, 98/77 and 98/82 are attributed to Paraves, MPZ 98/78–98/81 and 2022/84 are classified as *Buitreraptor*, and MPZ 2019/189 as *Paronychodon*. Among the small denticulated teeth (see Systematic palaeontology section), MPZ 98/72, 98/73, 98/75 and 2022/82 are classified as *Richardoestesia* in at least two discriminant analyses (MPZ 2022/90 only in DA3), but also as basal theropods or noasaurids (Table 2). MPZ 98/74 is assigned to "*Ischisaurus*" or Dromaeosauridae, MPZ 2004/7 to a non-tyrannosaurid tyrannosauroid, MPZ 2022/83 to Dromaeosauridae, Neovenatoridae, or non-averostran Neotheropoda, and MPZ 2022/80 to *Atrociraptor*, non-averostran Neotheropoda, or Noasauridae.

5.2. Cladistic analyses

The first two cladistic analyses carried out using a constrained topology with all the terminal taxa recovered trees with similar topologies. When cf. *Paronychodon* sp. and cf. *Richardoestesia* sp. were scored as mesial teeth, 2700 MPTs (Most Parsimonious Trees) were recovered (Length L = 1326 steps, Consistency Index CI = 0.197, Retention Index RI = 0.464). In the strict consensus tree (Fig. 7A), the three abelisaurid morphotypes were recovered within Abelisauroidea (Abelisauridae indet. 1 in a polytomy with *Masiakasaurus*, *Noasaurus,* and *Limusaurus*; and Abelisauridae indet. 2 and Abelisauridae indet. 3 among Abelisauridae). The cf. *Richardoestesia* sp. morphotype appears at the base of Neotheropoda, forming a polytomy with other early-branching neotheropods (e.g. *Dracovenator*, *Dilophosaurus*) and other averostrans such as ceratosaurians and megalosauroids. Both Paraves morphotypes are recovered as a distinct clade, sister to the above-mentioned polytomy at the base of Neotheropoda. The cf. *Paronychodon* sp. morphotype is recovered at the base of a clade that comprises basal coelurosaurians, tyrannosauroids and compsognathids, forming a polytomy with *Dilong*. Finally, the Dromaeosauridae indet. morphotype is recovered within Dromaeosauridae, as an early-branching member of Eudromaeosauria. A similar scenario was recovered in the constrained analysis including all the morphotypes but scoring cf. *Paronychodon* sp. and cf. *Richardoestesia* sp. as lateral teeth. In this case, far fewer MPTs were recovered (30), but they still show features similar to the previous analysis (L = 1326 steps, CI = 0.197, RI = 0.464). Both abelisaurid and dromaeosaurid morphotypes are recovered in the same positions as in the 'mesial' analysis, whereas the main difference concerns the position of the two Paraves, the cf. *Richardoestesia* sp. and the cf. *Paronychodon* sp. morphotypes. All four of these are recovered as a sister clade to Spinosauridae, with which the two Paraves and cf. *Paronychodon* sp. form a polytomy, whereas cf. *Richardoestesia* sp. represents a sister group to the clade formed by the other three taxa.

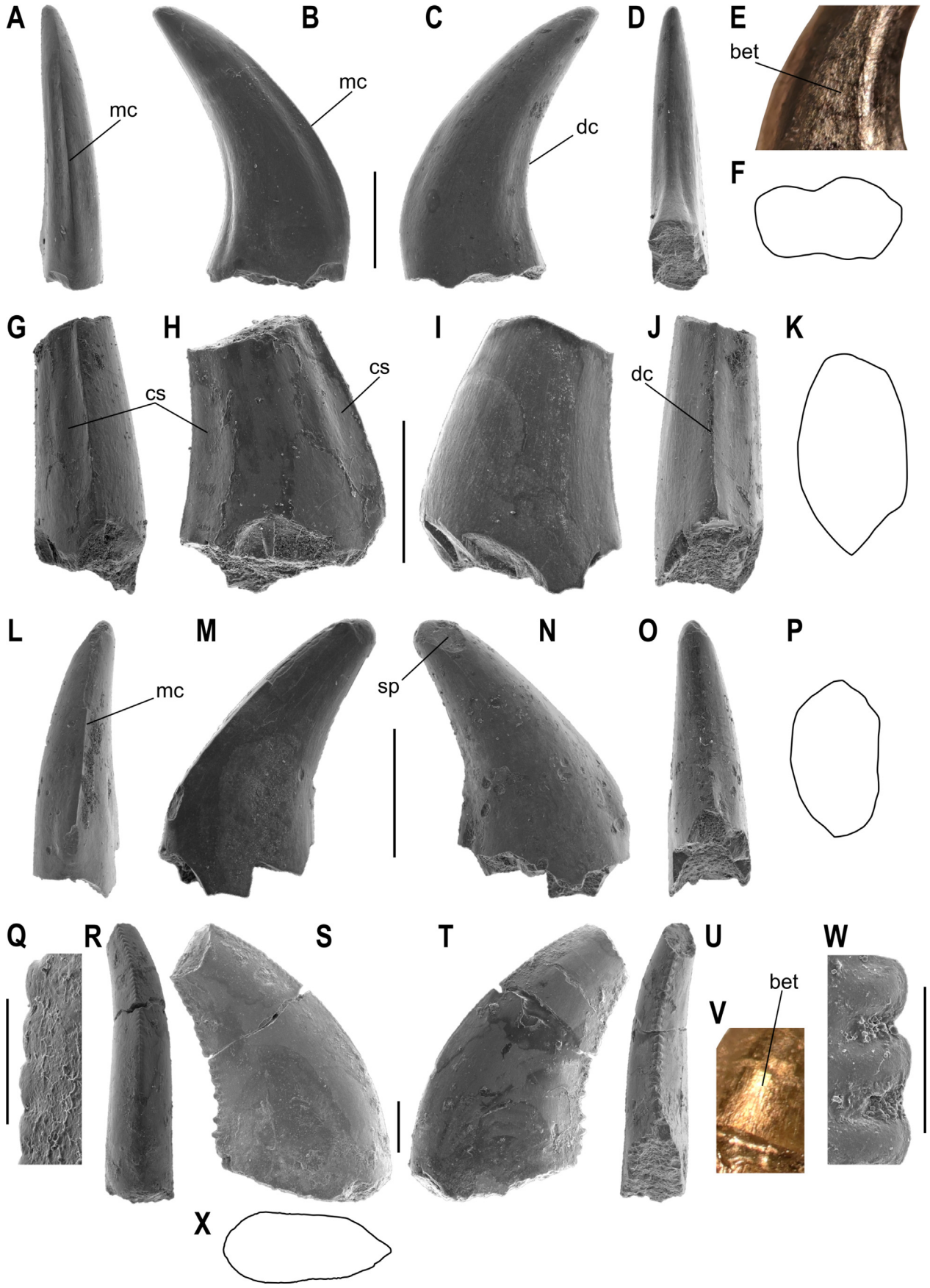
A
mc
B
mc
C
dc
D
E
bet
F
G
cs
H
cs
I
J
dc
K
L
mc
M
sp
N
O
P
Q
R
S
T
U
V
bet
W
X

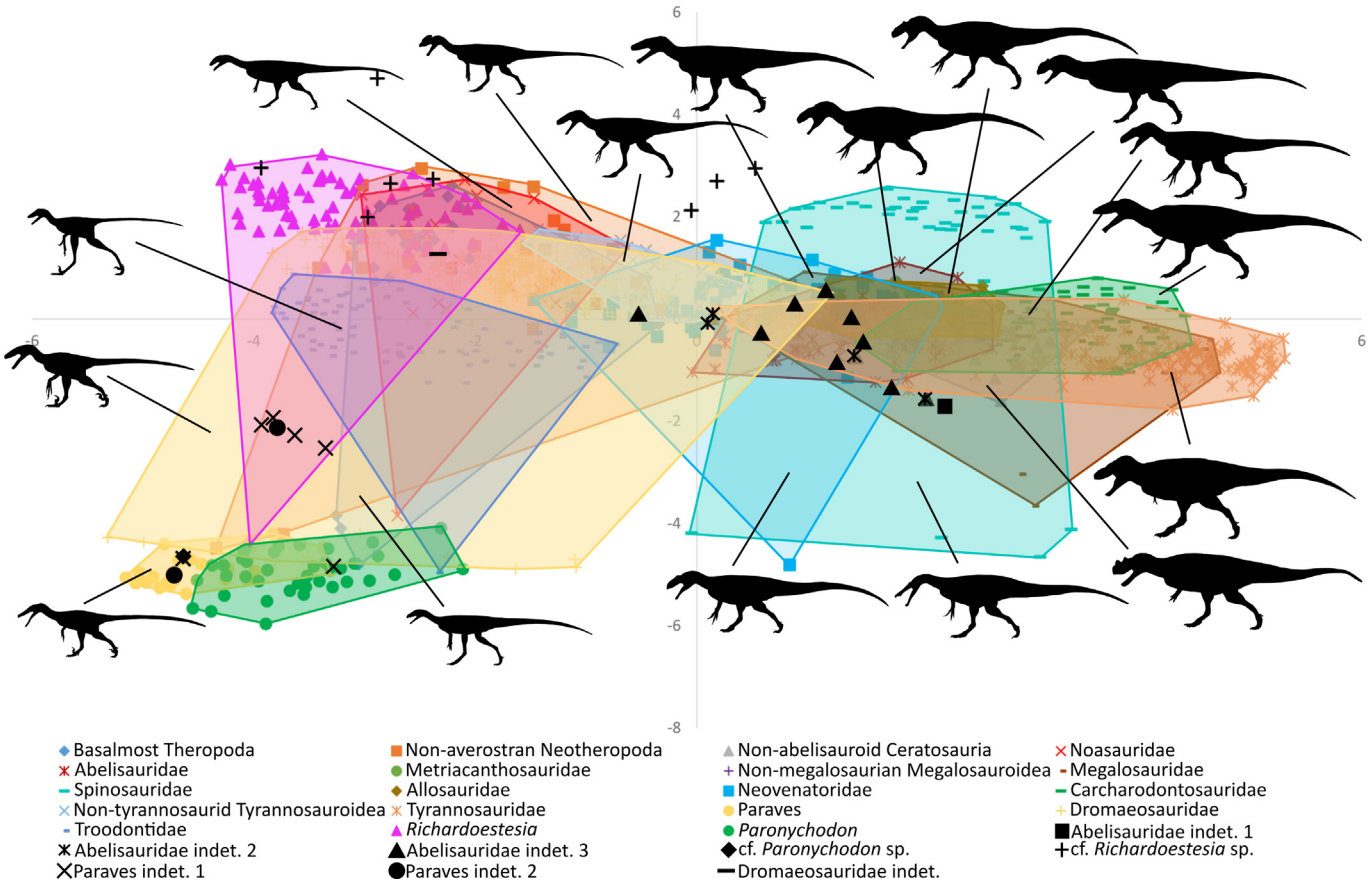

Fig. 6. Results of the discriminant analyses performed at group level. Discriminant analysis 2 (DA2) with five variables (CBL, CBW, CH, MC and DC). Silhouettes of *Richardoestesia* and *Paronychodon* were not added, due to their uncertain affinities within Theropoda. Silhouettes courtesy of Scott Hartman.

Table 1
Reclassification rate and percentages of variance of the discriminant analyses (DA1-DA4). Database in Supplementary material 1.

	Reclassification rate (%)	Variance (%)	
		Axis 1	Axis 2
DA1	46.68	73.68	17.48
DA2	54.84	71.19	21.53
DA3	49.54	72.02	15.88
DA4	56.35	69.45	20.14

Regarding the analyses with constraints performed with each of the OTUs considered separately, similar results were recovered for some of the morphotypes (Fig. 7B). The analysis with Abelisauridae indet. 1 yielded 5 MPTs (L = 1309 steps, CI = 0.199, RI = 0.473), in which the tooth is recovered within Abelisauroidea, among noasaurids, and combining with *Masiakasaurus*, *Noasaurus* and *Limusaurus*. In the case of Abelisauridae indet. 2, the analysis allowed just 2 MPTs to be recovered (L = 1309 steps CI = 0.199, RI = 0.473), with the tooth appearing in the consensus tree included within Abelisauridae, in a polytomy with *Majungasaurus* and *Indosuchus*. Abelisauridae indet. 3 was recovered as a sister taxon of *Majungasaurus*, among Abelisauridae, as the analysis found just 1 most parsimonious tree (L = 1309 steps, CI = 0.199, RI = 0.473). In the case of cf. *Paronychodon* sp., the analysis run with the morphotype scored as a mesial tooth provided 3 MPTs (L = 1312 steps, CI = 0.199, RI = 0.471), and this OTU was found to be either an early-branching tyrannosaurid, an early-branching neocoelurosaurian, or an early-branching compsognathid. For the 'lateral' scoring, the analysis yielded 4 MPTs (L = 1313 steps, CI = 0.199, RI = 0.471), with cf. *Paronychodon* sp. recovered as an early-branching ceratosaur (2 trees), as a non-neotheropod theropod (1 tree), or as an early-branching neotheropod, sister to *Dilophosaurus* (1 tree). Somewhat similar results were returned with the duplicated analyses of cf. *Richardoestesia* sp. The mesial version recovered 10 MPTs (L = 1308, CI = 0.200, RI = 0.473), classifying the morphotype as an early-branching averostran (3 trees), sometimes as a sister taxon to *Lilienstern*us, but also as a non-megalosaurian megalosauroid (1 tree), as a megalosaurid (3 trees), as a spinosaurid (2 trees), and as an early-branching avetheropod (1 tree). For the 'lateral' scoring, just 1 MPT (L = 1309, CI = 0.199, RI = 0.473) was recovered, resolving the position of cf. *Richardoestesia* sp. as a sister taxon to the clade Spinosauridae. For Paraves indet. 1, the analysis yielded 9

Fig. 5. Theropod teeth. A–K, Paraves indet. 1 morphotype. A–F, MPZ 98/77 in mesial, lingual, labial and distal views, enamel texture and basal cross-section scheme. G–K, MPZ 98/81 in mesial, lingual, labial and distal views, and basal cross-section scheme. L–P, Paraves indet. 2 morphotype. L–P, MPZ 98/82 in mesial, lingual, labial and distal views, and basal cross-section scheme. Q–X, Dromaeosauridae indet. morphotype. Q–X, MPZ 2022/80, mesial denticle close-up, mesial, lingual labial and distal views, enamel texture, distal denticle close-up, and basal cross-section scheme. Scale bars equal 1 mm, except for denticles and textures (0.3 mm). Abbreviations: bet, braided enamel texture; cs, concave surface; dc, distal carina; mc, mesial carina: sp, spalled surface.

Table 2
Results of the discriminant analyses (DA1-DA4) performed with the tooth sample studied in this work and the database. Database in Supplementary material 1.

	Discriminant analyses				
	Label	DA1	DA2	DA3	DA4
Abelisauridae indet. 1	MPZ 2004/4	*Abelisaurus*	Tyrannosauridae	*Abelisaurus*	Megalosauridae
Abelisauridae indet. 2	MPZ 2017/804	*Abelisaurus*	Abelisauridae	*Indosuchus*	Abelisauridae
Abelisauridae indet. 2	MPZ 2021/223	*Indosuchus*	Tyrannosauridae	*Abelisaurus*	Abelisauridae
Abelisauridae indet. 2	MPZ 2022/87	Unpublished dromaeosaurid	Allosauridae	Unpublished dromaeosaurid	Allosauridae
Abelisauridae indet. 2	MPZ 2022/88	*Abelisaurus*	Abelisauridae	*Abelisaurus*	Abelisauridae
Abelisauridae indet. 3	MPZ 98/67	*Dilophosaurus*	Tyrannosauridae	*Abelisaurus*	Megalosauridae
Abelisauridae indet. 3	MPZ 2004/3	*Dilophosaurus*	Abelisauridae	*Dilophosaurus*	Abelisauridae
Abelisauridae indet. 3	MPZ 2004/5	*Raptorex*	Neovenatoridae	Abelisauridae	Neovenatoridae
Abelisauridae indet. 3	MPZ 2004/6	Abelisauridae	Neovenatoridae	Abelisauridae	Neovenatoridae
Abelisauridae indet. 3	MPZ 2004/8	*Neovenator*	Abelisauridae	*Neovenator*	Abelisauridae
Abelisauridae indet. 3	MPZ 2022/81	Unpublished dromaeosaurid	Neovenatoridae	*Carnotaurus*	Neovenatoridae
Abelisauridae indet. 3	MPZ 2022/86	*Abelisaurus*	Abelisauridae	*Dubreuillosaurus*	Neovenatoridae
Abelisauridae indet. 3	MPZ 2022/89	*Raptorex*	Non-tyrannosaurid Tyrannosauroidea	*Deinonychus*	Non-tyrannosaurid Tyrannosauroidea
cf. *Paronychodon* sp.	MPZ 98/76	Paraves indet.	Paraves	Paraves indet.	Paraves
Paraves indet. 1	MPZ 98/77	Paraves indet.	Paraves	Paraves indet.	Paraves
Paraves indet. 1	MPZ 98/78	*Buitreraptor*			
Paraves indet. 1	MPZ 98/79	*Buitreraptor*			
Paraves indet. 1	MPZ 98/80	*Buitreraptor*			
Paraves indet. 1	MPZ 98/81	*Buitreraptor*			
Paraves indet. 1	MPZ 2019/189	cf. *Paronychodon*	*Paronychodon*	*Paronychodon*	*Paronychodon*
Paraves indet. 2	MPZ 98/82	Paraves indet.	Paraves	Paraves indet.	Paraves
Paraves indet. 2	MPZ 2022/84	*Buitreraptor*			
cf. *Richardoestesia* sp.	MPZ 98/72	*Eodromaeus*	*Richardoestesia*	*Richardoestesia*	
cf. *Richardoestesia* sp.	MPZ 98/73	cf. *Richardoestesia*	*Richardoestesia*	cf. *Richardoestesia*	*Richardoestesia*
cf. *Richardoestesia* sp.	MPZ 98/74	*Ischisaurus*	Dromaeosauridae	*Ischisaurus*	Dromaeosauridae
cf. *Richardoestesia* sp.	MPZ 98/75	*Richardoestesia*	*Richardoestesia*	*Richardoestesia*	*Richardoestesia*
cf. *Richardoestesia* sp.	MPZ 2004/7	*Proceratosaurus*	Non-tyrannosaurid Tyrannosauroidea	*Proceratosaurus*	Non-tyrannosaurid Tyrannosauroidea
cf. *Richardoestesia* sp.	MPZ 2022/83	Unpublished dromaeosaurid	Neovenatoridae	Unpublished dromaeosaurid	Non-averostran Neotheropoda
cf. *Richardoestesia* sp.	MPZ 2022/82	cf. *Richardoestesia*	Noasauridae	cf. *Richardoestesia*	Basalmost Theropoda
cf. *Richardoestesia* sp.	MPZ 2022/90	*Masiakasaurus*	Noasauridae	*cf. Richardoestesia*	Basalmost Theropoda
Dromaeosauridae indet.	MPZ 2022/80	*Atrociraptor*	Noasauridae	*Atrociraptor*	Non-averostran Neotheropoda

MPTs (L = 1309, CI = 0.199, RI = 0.473), recovering the morphotype in the consensus tree in a polytomy with *Chilesaurus*, *Berberosaurus* and *Dilophosaurus*, collapsing the clade Averostra. Paraves indet. 1 is classified as a non-averostran neotheropod (3 trees), as an early-branching ceratosaurian (5 trees), or as an early-branching tetanuran (1 tree). The analysis with only Paraves indet. 2 recovered 31 MPTs (L = 1311, CI = 0.199, RI = 0.472), the consensus of which resulted in a large polytomy that collapses several clades such as Neotheropoda, Ceratosauria, Tetanura, and Coelurosauria. Paraves indet. 2 shows great mobility, being recovered as non-averostran neotheropod, as an early-branching averostran, an early-branching ceratosaurian, an early-branching tetanuran, a sister taxon to *Chilesaurus*, an early-branching spinosaurid, an early-branching allosauroid, an early-branching coelurosaurian, or an early-branching neocoelurosaurian, sister taxon to *Ornitholestes* among others, eluding a precise phylogenetic classification. Finally, the analysis performed with Dromaeosauridae indet. recovered just one most parsimonious tree (L = 1310, CI = 0.199, RI = 0.472), this morphotype being nested within Dromaeosauridae as an early-branching eudromaeosaurian.

The analyses that were carried out without a constrained topology led to the classification of the studied morphotypes in large and unresolved polytomies. In the analysis in which cf. *Paronychodon* sp. and cf. *Richardoestesia* sp. were scored as mesial teeth, 2080 MPTs were recovered (L = 1082, CI = 0.241, RI = 0.587). In the strict consensus tree, Abelisauridae indet. 3, cf. *Richardoestesia* sp. and both Paraves (1 and 2) were recovered in a polytomy with *Ornitholesthes*, *Bicentenaria*, *Erectopus*, *Skorpiovenator*, *Chenanisaurus*, *Arcovenator*, *Noasaurus*, *Dilophosaurus*, *Dracovenator* and *Eodromaeus*. Abelisauridae indet. 1 was recovered in a polytomy with the two species of *Sinraptor*, nested in a clade with ceratosaurians, allosauroids and tyrannosaurids, whereas Abelisauridae indet. 2 appears as a sister taxon to *Indosuchus*, an abelisaurid. Dromaeosauridae indet. and cf. *Paronychodon* sp. were recovered in a polytomy with *Bambiraptor*, *Microraptor*, *Sinornithosaurus* and *Graciliraptor* (all four dromaeosaurians) but also with the juvenile *Limusaurus*. On the other hand, the analysis with cf. *Paronychodon* sp. and cf. *Richardoestesia* sp. interpreted as lateral teeth recovered more than 50000 MPTs (L = 1083, CI = 0.241, RI = 0.586), and the strict consensus tree collapsed into a large polytomy, with virtually all the studied morphotypes included. This polytomy brings together taxa ranging from early-branching theropods to dromaeosaurids, including ceratosaurians, abelisauroids, non-spinosaurid megalosaurids, allosauroids, tyrannosauroids, compsognathids and oviraptorosaurians. The only exception is Abelisauridae indet. 2, which appears again as a sister taxon to *Indosuchus*. All the strict consensus trees of each analysis can be found in Supplementary material 4.

6. Discussion

6.1. Taxonomic identification

Abelisauridae indet. morphotypes. The discriminant and cladistic analyses classify most of these teeth as Abelisauridae, but not necessarily referable to the Ibero-Armorican *Arcovenator* (Table 2). The cladistic analyses tend to recover both Abelisauridae indet. 2 and Abelisauridae indet. 3 as abelisaurids, reinforcing our

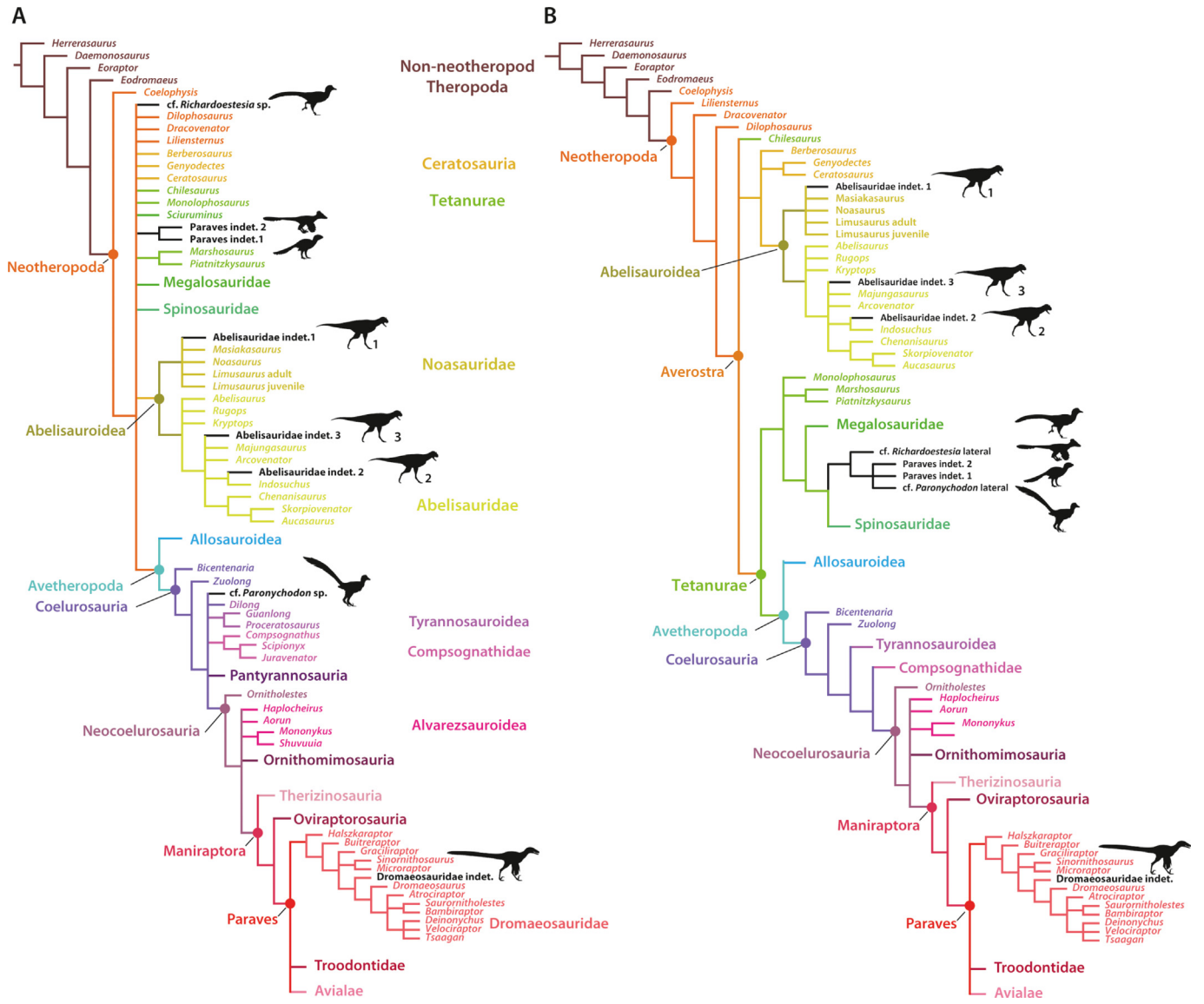

Fig. 7. Phylogenetic relationships of the eight morphotypes from the uppermost Maastrichtian Tremp Fm in the Western Tremp Syncline (Spain). A, simplified strict consensus tree from 2700 MPTs recovered from the cladistic analysis of the dentition-based data matrix from Meso et al. (2021) using a constrained search and all eight morphotypes, with cf. *Paronychodon* sp. and cf. *Richardoestesia* sp. scored as mesial teeth. B, simplified strict consensus tree from 30 MPTs recovered from the cladistic analysis of the dentition-based data matrix from Meso et al. (2021) using a constrained search and all eight morphotypes, with cf. *Paronychodon* sp. and cf. *Richardoestesia* sp. scored as lateral teeth. Silhouettes after Mette Aumala, Tasman Dixon, Rebecca Groom, Scott Hartman, and Emily Willoughby. For license attribution of the silhouettes, see Supplementary material 6.

morphology-based classification, whereas Abelisauridae indet. 1, placed among Noasauridae in the cladistic analysis with constrained topology, remains problematic. The synapomorphies for Noasauridae in this analysis are represented by 4 characters (29, 38, 44, 60), two of which (29 and 38) are not scored for Abelisauridae indet. 1, because they are related to the shape of the dentary alveoli and the presence of a constriction between root and crown, neither of which are preserved in MPZ 2004/4 (Fig. 3A–E). Having just one isolated specimen included in this morphotype, and one that is not well preserved, hindered the description of some features, and it was only possible to score the tooth for 18 of the 29 possible characters. This limitation, together with its large size, may reasonably challenge its phylogenetic classification within Noasauridae, as proposed by the analysis.

The combination of the following features permits the different Abelisauridae tooth morphotypes to be confidently assigned to Abelisauridae: the non-oriented and irregular enamel texture, the mostly straight or gently convex distal profile, denticulated mesial and distal carinae that reach the cervices or even extend beyond them, the denticle shape, the variation in denticle size along the carinae, and the DSDI values (see Hendrickx et al., 2020).

The only tooth assigned to Abelisauridae indet. 1 (MPZ 2004/4) is identified as mesial mainly on the basis of its cross-section as well as its asymmetrical labial and lingual surfaces (Hendrickx et al., 2015a). However, the CBR of this crown is less than 0.64, unlike the condition found in other ziphodont theropods. By contrast, the teeth grouped as Abelisauridae indet. 2 and 3 are identified as lateral due to their symmetrical cross-section profile. The teeth grouped within Abelisauridae indet. 2 exhibit a higher CBR, suggesting a more anterior location along the tooth row, whereas the Abelisauridae indet. 3 teeth probably correspond to more posterior maxillary or dentary teeth. As pseudoheterodonty is present in most theropods including the members of Abelisauridae (Hendrickx et al., 2019, 2020), it is likely that these abelisaurid morphotypes belong to the same taxon. However, as the abelisaurid record of the South Pyrenean Basin is currently limited, the

presence of more than one co-existing abelisaurid taxon cannot be ruled out either.

Most of the teeth from the Abelisauridae indet. 1, 2 and 3 morphotypes exhibit transverse undulations, a feature quite common in abelisaurids (e.g., Canale et al., 2009; Longrich et al., 2017; Hendrickx et al., 2020; Meso et al., 2021; Isasmendi et al., 2022), and an irregular enamel texture as in Abelisauridae (Hendrickx et al., 2019, 2020). As in Abelisauridae, in most of the Abelisauridae indet. teeth the denticles decrease in size near the cervix, and there is no notable size difference between the mid-crown and apicalmost denticles (Hendrickx et al., 2020). Furthermore, the DSDI values are close to 1, similar to the values observed in Abelisauridae (Hendrickx et al., 2020). Reminiscent of abelisaurid teeth, moreover, the teeth identified here as Abelisauridae indet. 1, 2 and 3 do not exhibit denticle densities higher than 20 denticles per 5 mm at mid-crown. Nevertheless, the observed denticle densities are usually quite high compared to other abelisaurid taxa, though still within the ranges of most abelisaurids except *Chenanisaurus* (see Longrich et al., 2017; Hendrickx et al., 2020).

The mesial crown of Abelisauridae indet. 1 also has denticulated mesial and distal carinae that seem to have reached at least the cervix, and a J-shaped basal cross-section like most abelisaurid mesial teeth (Fanti and Therrien, 2007; Smith, 2007; Hendrickx and Mateus, 2014; Hendrickx et al., 2020). The CBR of MPZ 2004/4 is within the range of the mesial teeth belonging to taxa such as *Abelisaurus*, *Rugops* and *Skorpiovenator* (Hendrickx et al., 2020). The distal profile of MPZ 2004/4 is somewhat concave, but nearly straight, so that the crown curves distally, as do the more distal crowns of the mesial dentition of Abelisauridae (Hendrickx et al., 2020). An apicobasally oriented concave surface adjacent to the carinae on the lingual surface is present in MPZ 2004/4, as in some abelisaurids (Hendrickx et al., 2020). The Abelisauridae indet. 1 crown also shares with abelisaurid mesial dentition the mesially facing mesial carina and the distally facing distal carina (Hendrickx et al., 2020), despite these not being specifically centrally placed. Indeed, the mesial carina is lingually displaced, whereas the distal one is labially deflected, differing from most abelisaurid mesial crowns (Hendrickx et al., 2020). Nevertheless, among Abelisauridae, the isolated abelisaurid mesial crown IIPG-09 and the lateral crowns of *Arcovenator*, at least, show labially displaced distal carinae (Hendrickx et al., 2020; Meso et al., 2021; Isasmendi et al., 2022).

The lateral crowns represented by Abelisauridae indet. 2 and 3 are low or moderately elongate but never reach a CHR of 2.3, like the lateral crowns of most abelisaurids (see Hendrickx et al., 2020). Almost all the lateral crowns of Abelisauridae indet. 2 and 3 have a straight or slightly concave distal profile like most abelisaurid teeth (Hendrickx et al., 2020), with the apex not extending beyond the basodistalmost point of the crown. Nevertheless, in MPZ 2004/6 and MPZ 2022/89, the concavity of the distal margin is more pronounced, and the apex extends further distally than the basodistalmost point of the crown in MPZ 2004/6, just as in *Arcovenator* (Hendrickx et al., 2020). The basal labiolingual compression of the Abelisauridae indet. 2 and 3 crowns is strong to moderate, as seen in most abelisaurids (see Hendrickx et al., 2020). Furthermore, the mesial and distal carinae of the studied crowns reach the cervix or extend below it as in Abelisauridae, but unlike *Arcovenator* (Hendrickx et al., 2019, 2020). Despite their similarities, however, most of the Abelisauridae indet. 2 and 3 teeth differ from most abelisaurid crowns in having uncentered mesial and distal carinae (see Hendrickx et al., 2020). Indeed, most of these teeth resemble those of *Arcovenator* in having a mesiolingually curving mesial carina and a strongly labially displaced distal carina. MPZ 2022/81 is the exception because its distal carina is somewhat twisted or bowed, like the condition reported in specimen IIPG-06 (Meso et al., 2021). The lateral dentition of Abelisauridae seems to be devoid of concave surfaces adjacent to the carinae (Hendrickx et al., 2020). However, they are present near the distal carinae on the lingual sides of MPZ 2004/8, MPZ 2017/804, and MPZ 2022/86. The orientation, shape and outline of the mesial and distal denticles of the Abelisauridae indet. 2 and 3 specimens are also consistent with other abelisaurid teeth (see Hendrickx et al., 2020). Interdenticular sulci are present in the Abelisauridae indet. 2 and 3 morphotypes, as in other abelisaurids (Hendrickx et al., 2020).

Despite the similarities with the dentition of *Arcovenator*, the Abelisauridae indet. 2 and 3 lateral teeth differ from *Arcovenator*, for instance in having a mesial carina that extends further basally and in the distal curvature of the crown, which is more pronounced in *Arcovenator* (e.g., Tortosa et al., 2014; Hendrickx et al., 2020; Isasmendi et al., 2022). Contrary to Pérez-García et al. (2016), therefore, these teeth are here assigned to an indeterminate abelisaurid other than *Arcovenator*.

Cf. Paronychodon sp. morphotype. The discriminant analyses classified specimen MPZ 98/76 as Paraves (Table 2) due to its small size and lack of denticles. However, this specimen exhibits longitudinal grooves and ridges (*sensu* Hendrickx et al., 2015a), differentiating it from other paravian teeth. The cladistic analyses show great variability in the possible phylogenetic positions for the cf. *Paronychodon* sp. morphotype from the Pyrenees, which is recovered within several different clades depending on the analysis. Some of these are implausible, such as basal Neotheropoda or basal Ceratosauria, and in general these analyses do not shed light on the phylogenetic affinities of the taxon. However, it is interesting to note that in the analysis of just this morphotype scored as a mesial tooth, it is always recovered within Coelurosauria, albeit nested within two clades that appear equally unlikely: Tyrannosauridae and Compsognathidae. Although the affinities of *Paronychodon* are unclear because the taxon is mostly represented by isolated teeth, there is currently a consensus that it is a coelurosaurian, but it is not clear whether it is a paravian, a dromaeosaurid, a troodontid, or something else (Currie et al., 1990; Larson, 2008; Sues and Averianov, 2013; Isasmendi et al., 2022). Given our poor knowledge of this taxon, it is thus understandable that its position in the different trees is not consistent.

MPZ 98/76 is without denticles, like most previously assigned *Paronychodon* teeth, including the *Paronychodon lacustris* holotype specimen (Cope, 1876; Currie et al., 1990), although some teeth assigned to *Paronychodon* bear denticles on the distal carina, or even on both carinae (Currie et al., 1990). Only the lingual surface of specimen MPZ 98/76 is flat, with three longitudinal grooves delimited by three longitudinal ridges (*sensu* Hendrickx et al., 2015a) as in other *Paronychodon* teeth (Cope, 1876; Currie et al., 1990; Canudo and Ruiz-Omeñaca, 2003). The planar lingual surface makes the basal cross-section of *Paronychodon* semicircular (Cope, 1876), similar to the reniform basal outline of cf. *Paronychodon* sp. from Laño and of MPZ 98/76 (Isasmendi et al., 2022, this work) or the D-shaped basal cross-section of the referred morphotype from Gams (Ősi et al., 2019). Although some of the North American denticulated teeth formerly assigned to *Paronychodon* overlap with the premaxillary teeth of *Bambiraptor* and *Saurornitholestes* (Currie and Evans, 2020), MPZ 98/76 does not seem to be a premaxillary tooth from an Iberian dromaeosaurid similar to those from North America, because this specimen is undenticulated.

MPZ 98/76 is similar to some of the morphotype IV teeth of *Paronychodon asiaticus* from the Cenomanian–Turonian Bissekty and Khodzhakul formations of Uzbekistan (Nessov, 1995; Sues and Averianov, 2013), because these lack denticles and exhibit similar groove arrangement patterns, with lateral surfaces that lack this ornamentation, and a flat lingual surface with a similar number of

grooves. However, whereas the distal carina is usually lingually located in this morphotype (Sues and Averianov, 2013), in MPZ 98/76 it is centrally placed.

Tooth MPZ 98/76 from the South Pyrenean Basin is similar to previously reported European *Paronychodon* teeth in the outline of the crown base, the flat lingual surface, and the undenticulated carinae. Nevertheless, it differs from most of the previously referred crowns because it lacks grooves/ridges on the labial surface, similar to the teeth from the Turonian locality of Gams (Austria) and the Maastrichtian locality of Nălaţ-Vad (Romania) (Smith et al., 2002; Ősi et al., 2019). MPZ 98/76 shares with the crown from Gams the number of grooves, but these seem to be shallower on the latter specimen. Despite the similarities with some teeth referred to the North American *P. lacustris*, the Asian *P. asiaticus*, and other European specimens, the lack of fossil material other than isolated teeth prevents MPZ 98/76 from being confidently attributed to any of these nominal species or even to the genus. Considering these limitations, therefore, MPZ 98/76 is here assigned to cf. *Paronychodon* sp.

Cf. Richardoestesia sp. morphotype. Most of the teeth within this morphotype have been classified as *Richardoestesia* (Table 2) in at least one of the discriminant analyses carried out, supporting their referral to this genus. As happens with *Paronychodon*, however, this tooth morphotype is problematic owing to its uncertain phylogenetic affinities (Currie et al., 1990), and it has even been proposed that *Paronychodon* and *Richardoestesia* might represent different teeth from the same taxon (Longrich, 2008) that exhibit differences due to heterodonty. Against this background, the poor performance of cf. *Richardoestesia* sp. in the cladistic analyses is again understandable, where it is recovered within the clade Megalosauroidea, sometimes within Spinosauridae, or even as an early-branching neotheropodan. These positions are usually driven by the characters coding a serrated distal carina (49 → 0) or the extension of the serration of the mesial carina to the cervix (51 → 1), but also by character 54, which could not be scored for *Richardoestesia.* It is noteworthy that Hendrickx et al. (2019) removed *Richardoestesia gilmorei* from a previous version of the data matrix used here, having ascertained that the taxon is difficult to place in a constrained analysis.

The teeth grouped within the cf. *Richardoestesia* sp. morphotype are small like the teeth of *Richardoestesia*, have a virtually identical braided enamel texture, and are more reminiscent of the North American *Richardoestesia isosceles* or the Asian *Richardoestesia asiatica* in being relatively elongate and in having rather straight crowns (Currie et al., 1990; Sankey et al., 2002; Sues and Averianov, 2013; Averianov and Sues, 2019). Although plenty of *Richardoestesia* crowns from other sites exhibit oval or figure-eight-shaped basal cross-sections (e.g., Larson, 2008; Hendrickx and Mateus, 2014; Isasmendi et al., 2022), most of the studied teeth have a reniform basal cross-section, a feature also present, for instance, in some North American specimens (e.g., Sankey et al., 2002, fig. 5; Willianson and Brusatte, 2014, fig. 8) or in some crowns of *R. asiatica* (e.g., Averianov and Sues, 2019, fig. 4v).

Richardoestesia crowns are characterized by the possession of minute denticles (more than 5 or 6 denticles per mm) on the distal carinae (Currie et al., 1990; Hendrickx et al., 2019). This is similar to the denticle densities found in the cf. *Richardoestesia* sp. morphotype, which indeed has even higher denticle densities (8–13 denticles per 1 mm, or 40–65 denticles per 5 mm). Half of the studied specimens with preserved mesial carinae have denticles whereas the other half lack them, a feature also present in other samples of *Richardoestesia* teeth (e.g., Sankey et al., 2002; Torices et al., 2015; Averianov and Sues, 2019). The mesial denticles of the cf. *Richardoestesia* sp. morphotype are subquadrangular or slightly apicobasally subrectangular. The distal denticles are more proximodistally subrectangular. This denticle shape is consistent with that of *R. isosceles*, whereas the denticles are not as subquadrangular in *Richardoestesia gilmorei*, and furthermore these have small interdenticular spaces unlike in *R. asiatica* and *R. isosceles* (Sankey et al., 2002; Averianov and Sues, 2019). Diverging from the typical condition found in most theropods at least, the teeth attributed to *R. isosceles* from the uppermost Santonian Milk River Fm and most of the *R. asiatica* specimens from the upper–middle Turonian Bissekty Fm seem to display random changes in denticle size along the carinae (Larson, 2008; Averianov and Sues, 2019). This variation is also recorded along the mesial carinae of MPZ 2004/7 and MPZ 2022/82. In *Richardoestesia*, the distal carinae are strongly labially displaced (Hendrickx et al., 2019). Although the distal carina of MPZ 98/75 is similarly placed, its deflection is less pronounced. In the other specimens where the position of the distal carina can be assessed, it is centered, as in both cf. *Richardoestesia* sp. morphotypes described from the upper Campanian Laño site (Isasmendi et al., 2022).

Averianov and Sues (2019) distinguished five morphotypes among *R. asiatica* based mainly on the crown morphology, despite an overlap in terms of the CBR and CHR, as well as the crown- and denticle-shape and disposition. Of these morphotypes, the Spanish specimens MPZ 98/74 and MPZ 2004/7 resemble morphotype A or the less distally recurved specimens of morphotype C in having a more convex or straight distal margin and not being as recurved. Specimens MPZ 98/72, MPZ 98/73, MPZ 2022/82 and MPZ 2022/90 are similar to the teeth belonging to morphotype C and the most elongate teeth of morphotype D, because they are relatively elongate and have a more convex distal margin. Finally, MPZ 98/75 is like the teeth of morphotype E and the shorter specimens of morphotype C in being lower, slightly distally recurved, and having an almost straight distal margin (see Averianov and Sues, 2019).

The European *Richardoestesia*-like teeth exhibit remarkable variability in crown-shape, curvature, and the presence or absence of mesial denticles. Nevertheless, they are small in size, have tiny denticles, and have DSDI values $\geq$1 in the specimens with denticulated mesial carinae (see, e.g., Codrea et al., 2002; Valentin et al., 2012; Vasile et al., 2012; Ortega et al., 2015; Csiki-Sava et al., 2016; Marmi et al., 2016; Isasmendi et al., 2022; this study). The teeth of our cf. *Richardoestesia* sp. morphotype resemble the cf. *Richardoestesia* sp. B teeth from Laño (Isasmendi et al., 2022) in the overall crown-shape, the extension and disposition of the carinae, the possession or absence of denticles, and their densities. However, MPZ 2004/7 and MPZ 2022/82 have sporadic denticle-size variation. The Laño teeth seem to have an irregular enamel texture, whereas this is braided on the better-preserved crowns studied herein, although the former could simply be abraded. Further similar teeth are present in several other European sites as well (e.g., Buffetaut et al., 1986, drawing d; Codrea et al., 2002, fig. 4L; Codrea et al., 2013, plate I-21; Vasile, 2008, fig. 2o; Ortega et al., 2015, fig. 7D).

Despite the aforementioned similarities between our South Pyrenean teeth and other *Richardoestesia* or closely related teeth, as well as the high-confidence classification of these teeth as *Richardoestesia* by the discriminant analyses, the European fossil record of this genus is still poor, hindering the confident assignment of these teeth to *Richardoestesia*. The teeth MPZ 98/72, MPZ 98/73, MPZ 98/74 and MPZ 2004/7, which were previously attributed to ?*Richardoestesia* sp. by Torices et al. (2015), specimen MPZ 98/75, identified as *Nanoraptor pyrenaicus* by Torices (2007), and the three other teeth in this sample are therefore here assigned to cf.

Richardoestesia sp., being most similar to *R. asiatica*, *R. isosceles*, cf. *Richardoestesia* sp. B from Laño, or to other similarly elongate European teeth.

Paraves indet. morphotypes. All the teeth except MPZ 2019/189 were classified as *Buitreraptor* or Paraves by the discriminant analyses (Table 2). MPZ 2019/189 was instead attributed to *Paronychodon* (Table 2), although it lacks any longitudinal grooves or ridges (*sensu* Hendrickx et al., 2015a). Therefore, these analyses support the affinities of the teeth with other paravians overall. By contrast, the cladistic analyses performed with the two Paraves morphotypes do not support their assignation within that clade very well, as their position varies greatly in the different MPTs, and they were never recovered within the Paraves clade. Since the state of knowledge of Late Cretaceous paravian theropods from Europe is poor and mostly based on isolated elements, it is reasonable to conclude that they are underrepresented in the data matrix, so it may be difficult to recover them in their respective clades. More complete material is needed to compare and score these taxa properly.

The South Pyrenean teeth grouped within Paraves indet. 1 and 2 are asymmetrical, distally recurved, ziphodont, and have no constriction between the crown and root. Furthermore, the combination of the lack of denticles on the mesial and distal carinae, their small size, their CH values still higher than 1, and CBR values lower than 0.75, suggests paravian affinities for these tooth morphotypes (Hendrickx et al., 2019).

The teeth of paravian theropods (Dromaeosauridae + Troodontidae + Avialae, according to Sereno, 1997) exhibit a wide range of variation (e.g., Currie et al., 1990; Sankey et al., 2002; Hendrickx et al., 2019; Currie and Evans, 2020). Undenticulated teeth are found in many paravians (Hendrickx et al., 2019 and references therein), and in fact this condition could be apomorphic for Paraves (Hendrickx et al., 2019). Among paravians, many taxa have concave surfaces on their mesial dentition (Hendrickx et al., 2019), as seen in specimens MPZ 98/77, MPZ 98/79 and MPZ 98/81.

The dentition is folidont in anchiornithines and jinfengopterygines (Hendrickx et al., 2019), unlike the ziphodont teeth studied herein. However, lateral ziphodont dentition is also present in *Jinfengopteryx*, *Byronosaurus*, *Gobivenator*, and *Xixiasaurus* (Makovicky et al., 2003; Xu and Norell, 2004; Averianov and Sues, 2007; Lü et al., 2010; Tsuihiji et al., 2014; Hendrickx et al., 2019). The teeth of *Byronosaurus* and *Xixiasaurus* have a figure-eight-shaped basal cross-section (Hendrickx et al., 2019), as does MPZ 98/77. Moreover, the basal outline of some lateral teeth of *Byronosaurus* is also elliptical (Makovicky et al., 2003), similar to MPZ 98/78.

Among Dromaeosauridae, the teeth of halszkaraptorines and unenlagiines except *Austroraptor* are strongly distally recurved, with lateral ziphodont teeth (Novas et al., 2009; Gianechini et al., 2011a; Cau et al., 2017; Hendrickx et al., 2019), similar to the specimens studied here. The latter, however, differ from the teeth of unenlagiines in not possessing ridged/fluted lateral teeth and, at least from *Buitreraptor*, also in not having mesial carinae and in most of the teeth exhibiting lower CBR values (see Novas et al., 2009; Gianechini et al., 2011a; Hendrickx et al., 2019). Nevertheless, MPZ 98/77 has a figure-eight-shaped cross-section, like the lateral teeth of *Buitreraptor* (Gianechini et al., 2011a; Hendrickx et al., 2019). The halszkaraptorine *Halszkaraptor* has constrictions between the root and crown, and possibly all halszkaraptorines have D-shaped mesial teeth (Hendrickx et al., 2019), unlike the Pyrenean teeth grouped in these morphotypes. Some mesial and lateral teeth of microraptorines are not denticulated and ziphodont (Hendrickx et al., 2019 and references therein), similar to Paraves indet. 1 and 2 identified here. Furthermore, a figure-eight-shaped cross-sectional outline is inferred to be present in *Graciliraptor*, *Microraptor*, and *Sinornithosaurus* (Gianechini et al., 2011b; Hendrickx et al., 2019).

At least some of the Paraves indet. 1 and 2 teeth seem to have a braided enamel texture, as do many eudromaeosaurs (Hendrickx et al., 2019). This condition differs from that found in the troodontids *Byronosaurus* and *Troodon*, as well as in the dromaeosaurids *Buitreraptor*, *Tsaagan*, *Velociraptor*, and the lateral teeth of *Dromaeosaurus*, all of which have an irregular tooth enamel texture (Hendrickx et al., 2019).

The teeth of the Ibero-Armorican *Pyroraptor* are denticulated (Allain and Taquet, 2000) and so differ from the paravian teeth studied in this work. By contrast, non-denticulated paravian teeth have been described in other Ibero-Armorican sites (Antunes and Sigogneau-Russell, 1992; Sigé et al., 1997; Garcia et al., 2000; Company et al., 2009; Torices et al., 2015; Isasmendi et al., 2022). The degree of elongation and curvature of the teeth belonging to Paraves indet. 1 is like those from Aveiro, Fons-Champ-Garimond, La Neuve, Montrebei, Vicari-4 and at least three teeth from Taveiro (TV 23, 26 and 30) (see Antunes and Sigogneau-Russell, 1992; Sigé et al., 1997; Garcia et al., 2000; Torices et al., 2015). The teeth from Paraves indet. 2 are more similar to TV 28 and 29 from Taveiro (see Antunes and Sigogneau-Russell, 1992).

The specimens studied herein share the following features with the Laño teeth belonging to Paraves indet. (Isasmendi et al., 2022): undenticulated mesial and distal carinae that reach the cervix or nearly do so, centered distal carinae on most crowns, some crowns with slightly lingually displaced mesial carinae, lack of ornamentation, and no constriction between root and crown. The Paraves indet. 1 teeth are similarly recurved and elongated, like many teeth belonging to the Paraves indet. A morphotype. Furthermore, the elliptical basal cross-section of MPZ 98/78 and the more oval-shaped cross-sectional outline of MPZ 2019/189 and MPZ 98/80 do not differ significantly from the Paraves indet. A morphotype from Laño. Likewise, the Paraves indet. 2 crowns are low, like those of Paraves indet. B, and MPZ 98/82 exhibits a reniform basal cross-section, like many of the Paraves indet. B teeth from Laño. The consistent differences between the two morphotypes can be interpreted as indicating that they belong to two different taxa or as being due to dental variability along the tooth row, since the latter phenomenon occurs widely among Theropoda (Hendrickx et al., 2019 and references therein).

Specimens MPZ 98/77 and MPZ 98/78 were previously assigned to ?*Paronychodon* sp. by Torices et al. (2015). Despite these teeth being undenticulated, like those of *Paronychodon lacustris* (Cope, 1876) and other teeth assigned to the genus, they lack the characteristic longitudinal ridges/grooves of the genus *Paronychodon* and hence cannot be assigned to it. Therefore, taking into consideration the poor European theropod fossil record, the differences noted with respect to the dentition of other small-toothed non-paravian coelurosaurs, the wide range of dentition types occurring in Paraves, and the similarities of the teeth studied here with paravian teeth from other Ibero-Armorican sites, the teeth MPZ 98/79-MPZ 98/81 (previously assigned to Coelurosauria indet. by Torices et al., 2015), MPZ 98/77-MPZ 98/78 and MPZ 2019/189 are here assigned to Paraves indet. 1, whereas specimens MPZ 98/82 (previously assigned to Coelurosauria indet. by Torices et al., 2015) and MPZ 2022/84 are attributed to Paraves indet. 2.

Dromaeosauridae indet. morphotype. Two of the discriminant analyses carried out classified specimen MPZ 2020/80 as *Atrociraptor*, and the other two as belonging to Noasauridae or as a non-averostran neotheropod. The cladistic analyses support its assignation as a dromaeosaurid tooth well, Dromaeosauridae being the only clade where this morphotype is consistently recovered.

Like many dromaeosaurid teeth, specimen MPZ 2020/80 is small and ziphodont, bears mesial and distal carinae that are both denticulated, and has an especially high DSDI value exceeding 1.2 (Hendrickx, 2015; Hendrickx et al., 2019). Specimen MPZ 2020/80 also shares with Dromaeosauridae the lack of constriction between the crown and root and a very pronounced concave distal profile (Hendrickx et al., 2019). A figure-eight-shaped basal cross-section similar to that of MPZ 2022/80 also appears in most dromaeosaurids but also in other theropod taxa (Hendrickx et al., 2019). The braided enamel texture present on the crown surface of MPZ 2022/80 is also widely distributed among Theropoda and is present in eudromaeosaurians (Hendrickx et al., 2019).

Denticles are present in some microraptorine teeth, all the lateral teeth of Dromaeosaurinae, and some lateral teeth of velociraptorines (Hendrickx et al., 2019). The usual denticle-shape of dromaeosaurid teeth is subrectangular and chisel-like (Currie et al., 1990; Torices et al., 2015), and most dromaeosaurines and velociraptorines, as well as all microraptorines where denticles are present, exhibit symmetrically to asymmetrically convex denticles (Hendrickx et al., 2019), as seen in MPZ 2022/80. Its distal denticles are also similar to those of dromaeosaurids in being proximodistally subrectangular (Hendrickx et al., 2019).

Specimen MPZ 2022/80 has a planar surface in the lingual surface near the distal carina. Concave or planar surfaces adjacent to carinae appear in many theropod clades, notably on the mesial dentition of many paravians (Hendrickx et al., 2019). Taken together, this combination of features allows specimen MPZ 2022/80 to be assigned to Dromaeosauridae indet.

Within the Ibero-Armorican fossil record, a number of dromaeosaurid remains, especially teeth, have been reported from both Lower and Upper Cretaceous sites (e.g., Ortega et al., 2015; Torices et al., 2015; Fuentes-Vidarte et al., 2016; Marmi et al., 2016; Alonso et al., 2017), although *Pyroraptor* is the only nominal dromaeosaurid described with preserved teeth (Allain and Taquet, 2000). As with the South Pyrenean tooth, the tooth crowns of *Pyroraptor* have a figure-eight-shaped basal cross-section, and DSDI values higher than 1.2 (Hendrickx et al., 2019). The denticle densities are also similar between MPZ 2022/80 and the *Pyroraptor* specimens MNHN BO014 and BO015. Nonetheless, the mesial denticles extend further basally in *Pyroraptor* compared to MPZ 2022/80. Furthermore, the disposition of the mesial and distal carinae is different in MPZ 2022/80 from the *Pyroraptor* teeth. Whereas in MPZ 2022/80 the mesial carina is slightly lingually displaced, in *Pyroraptor* teeth it is centered. The distal carina of MPZ 2022/80 is centrally located. In *Pyroraptor*, by contrast, this seems to be bowed labially. In addition, MNHN BO014 and BO015 show well-developed, distally positioned, concave surfaces adjacent to the distal carinae. In MPZ 2022/80 a planar surface can be seen in this position, instead.

Compared with other Iberian dromaeosaurid teeth, MPZ 2022/80 exhibits denticles that are perpendicular to the carinae, unlike the velociraptorine crowns from Lo Hueco, which have apically inclined denticles (Ortega et al., 2015). The dromaeosaurine teeth from Lo Hueco also exhibit larger denticles, and hence lower density values compared to MPZ 2022/80. Furthermore, MPZ 2022/80 is more distally recurved and has higher denticle densities compared to the teeth assigned to cf. Dromaeosauridae recovered from Figuerola 2 and Fontllonga 6 (Torices et al., 2015). On the other hand, specimen MPZ 2022/80 shares with the Laño dromaeosaurid teeth the enamel texture, the overall crown shape, the basal cross-section, the position and extension of both carinae, the overall denticle shape, and the denticle densities. However, the Laño dromaeosaurid teeth lack the planar surface adjacent to the distal carinae (Isasmendi et al., 2022).

In the light of these considerations as well as given the classification of this tooth as *Atrociraptor* by DA1 and DA3, MPZ 2022/80 is here identified as Dromaeosauridae indet. Although they belong to the same family, however, MPZ 2022/80 has features differentiating it from *Pyroraptor* and from the dromaeosaurid teeth from the Figuerola 2, Fontllonga 6, Laño and Lo Hueco sites.

6.2. Theropod palaeobiodiversity in the upper Maastrichtian of the Western Tremp Syncline and the intra-Maastrichtian faunal turnover of Ibero-Armorican theropods

A comparable previous study carried out in the Western Tremp Syncline recognized six theropod tooth morphotypes (Torices et al., 2015): Theropoda indet. morphotype 1 and 2 (regarded as cf. *Arcovenator* by Pérez-García et al., 2016), Coelurosauria indet., ? *Paronychodon* sp., ?*Richardoestesia* sp., and ?Dromaeosauridae indet. In the present work, the indeterminate theropod morphotypes and the cf. Dromaeosauridae indet. (MPZ 2004/6) of Torices et al. (2015) are assigned to Abelisauridae indet. 1, 2 and 3, instead. As in Torices et al. (2015), in this study only one cf. *Richardoestesia* sp. morphotype has been found. As previously, specimen MPZ 98/76 is also attributed to cf. *Paronychodon* sp., but MPZ98/77 and MPZ98/78 (?*Paronychodon* sp. in Torices et al., 2015) are here referred to Paraves indet. 1. The Coelurosauria indet. morphotype is here attributed to two paravian morphotypes (Paraves indet. 1 and 2), and with a previously undescribed specimen, a new Dromaeosauridae indet. morphotype is proposed. In this study, we therefore identify eight tooth morphotypes: Abelisauridae indet. 1, 2 and 3, Dromaeosauridae indet., Paraves indet. 1 and 2, cf. *Paronychodon* sp., and cf. *Richardoestesia* sp. Aside from this, the presence of an ornithuromorph avialan vertebra from the area (Pérez-Pueyo et al., 2021b) increases the number of theropod taxa in the Western Tremp Syncline to a minimum of six.

A latest Cretaceous faunal change first identified in the Ibero-Armorican domain by Le Loeuff et al. (1994) was later studied in detail by several authors, especially for non-theropod dinosaurs (see Vila et al., 2016; Fondevilla et al., 2019 and references therein). This event was first proposed to have occurred in a relatively short time span in the early late Maastrichtian, around the C31r–C31n reversal (Vila et al., 2016). However, Fondevilla et al. (2019) concluded that the faunal turnover would have been a longer process that started in the early Maastrichtian and ended in the early late Maastrichtian, lasting for around 2.5–2.8 Ma between the lower part of chron C31r and the C30r/C30n boundary (Fig. 8). Herein, the time span from Fondevilla et al. (2019) is accepted.

Since uppermost Cretaceous theropod remains are scarce and mainly consist of isolated teeth, it is difficult to study the impact that the intra-Maastrichtian faunal turnover had on this dinosaur group. Prior studies have not found significant changes in the composition of theropod faunas during this interval and have maintained that this event would not have affected the non-avian theropods (Torices et al., 2015; Vila et al., 2016; Fondevilla et al., 2019; Isasmendi et al., 2022; Malafaia et al., 2023). However, the more thorough study and revision carried out herein is the most specific approach made until now to assessing the theropod faunas during the intra-Maastrichtian faunal turnover. Nevertheless, it is worth pointing out that there are different numbers of pre-turnover, intra-turnover, and post-turnover theropod-bearing sites that are more or less accurately dated, with more sites dated to the pre-turnover than to the post-turnover period, and very few

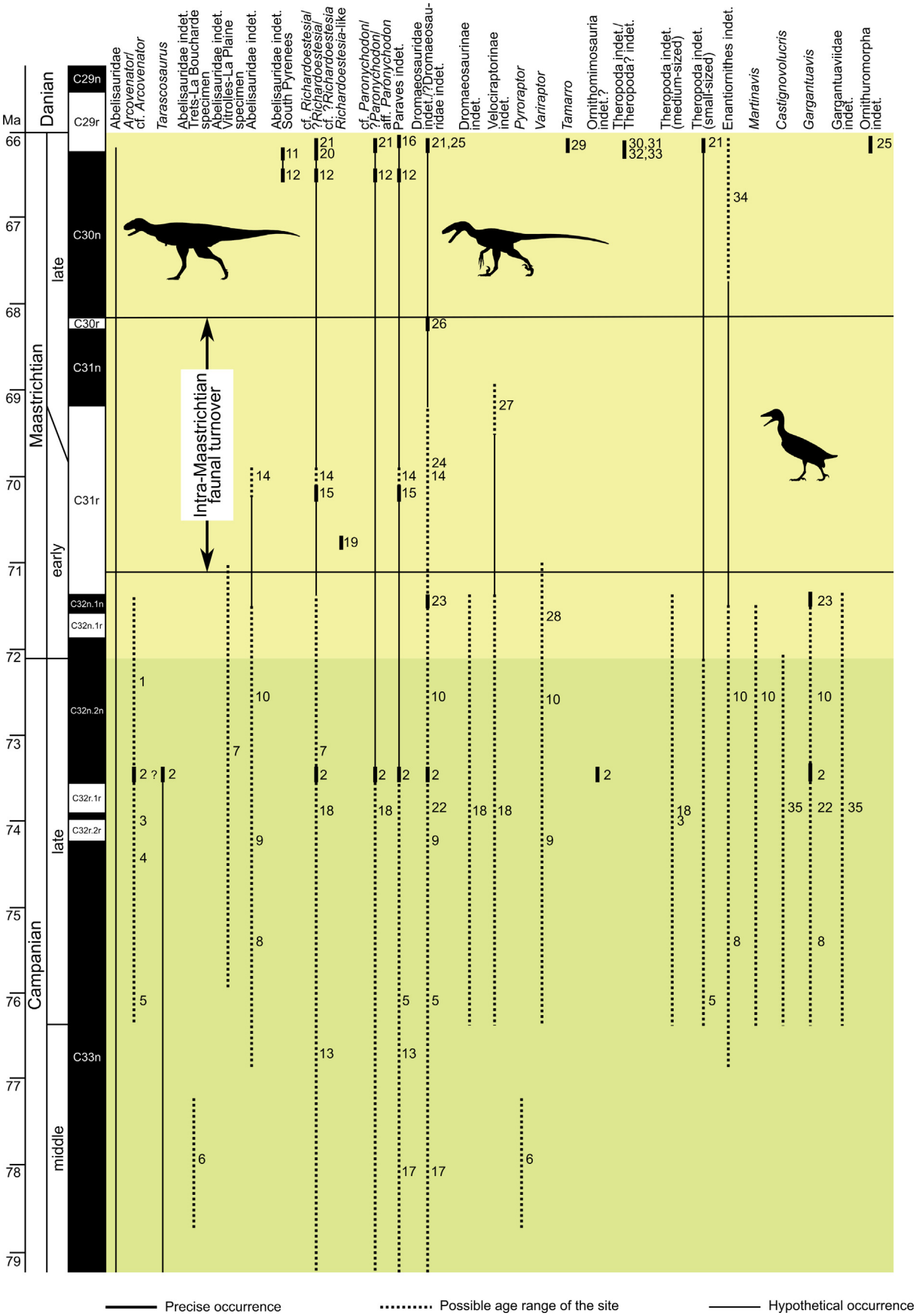
Abelisauridae
Arcovenator/ cf. Arcovenator
Tarascosaurus
Abelisauridae indet. Trets-La Boucharde specimen
Abelisauridae indet. Vitrolles-La Plaine specimen
Abelisauridae indet.
Abelisauridae indet. South Pyrenees
cf. Richardoestesia/ ?Richardoestesia/ cf. ?Richardoestesia
Richardoestesia-like
cf. Paronychodon/ ?Paronychodon/ aff. Paronychodon
Paraves indet.
Dromaeosauridae indet./?Dromaeosauridae indet.
Dromaeosaurinae indet.
Velociraptorinae indet.
Pyroraptor
Variraptor
Tamarro
Ornithomimosauria indet.?
Theropoda indet./ Theropoda? indet.
Theropoda indet. (medium-sized)
Theropoda indet. (small-sized)
Enantiornithes indet.
Martinavis
Castignovolucris
Gargantuavis
Gargantuaviidae indet.
Ornithuromorpha indet.
Ma
Danian
Maastrichtian
Campanian
late
early
late
middle
C29n
C29r
C30n
C30r
C31n
C31r
C32n.1n
C32n.1r
C32n.2n
C32r.1r
C32r.2r
C33n
Intra-Maastrichtian faunal turnover
Precise occurrence
Possible age range of the site
Hypothetical occurrence

sites from the turnover period itself. Thus, a sampling bias and sample-size factors cannot be ruled out (Supplementary material 5).

Assessment of the higher-level palaeobiodiversity for pre-turnover, intra-turnover, and post-turnover theropod faunas shows the same groups to be present in all three time slots: abelisaurid ceratosaurians, the enigmatic taxa cf. *Richardoestesia* and cf. *Paronychodon*, indeterminate paravians, dromaeosaurids, as well as large ornithuromorph avialans and enantiornithines. Nevertheless, representatives of Troodontidae occur solely in the post-turnover faunas, with *Tamarro insperatus* (Sellés et al., 2021) (Fig. 8).

A few abelisaurid taxa have been described from the Upper Cretaceous deposits of southern France, such as *Tarascosaurus salluvicus* (Le Loeuff and Buffetaut, 1991) and *Arcovenator escotae* (Tortosa et al., 2014). The lower and upper Campanian abelisaurid record is richer than the Maastrichtian. *Tarascosaurus* was defined from elements recovered from the lower Campanian 'Fuvelian' grey limestone (upper part of chron C33r; Fondevilla et al., 2016b) in Lambeau du Beausset of Provence (France) (Le Loeuff and Buffetaut 1991; Tortosa et al., 2014). Moreover, two femora from Laño (upper Campanian, chron C32n; Corral et al., 2016) in Treviño County (Burgos, Spain) have also been compared with this genus (Le Loeuff and Buffetaut, 1991; Le Loeuff, 1992), although the current whereabouts of these elements is unknown (Isasmendi et al., 2021). It is therefore not possible to reassess this material. *Arcovenator* was erected from material recovered from the upper Campanian–lower Maastrichtian of Pourrières-Jas Neuf Sud locality (Var Department, France) and is the most complete European abelisaurid recovered to date (Tortosa et al., 2014). Apart from the type locality, isolated teeth of this genus have also been found in the upper Campanian of the sites of Armuña (Segovia Province, Spain), Chera (Valencia Province, Spain), and Laño (Pérez-García et al., 2016; Isasmendi et al., 2022). In addition, in Armuña, the possible lateral side of the ungual phalanx UPUAM 14066 (Pérez-García et al., 2016) has a bifurcated lateral groove. This feature is present in abelisauroid theropods among early-branching averostrans (e.g., Novas and Bandyopadhyay, 2001; Carrano et al., 2002; Carrano and Sampson, 2008; Novas et al., 2013), and hence this element can be confidently attributed to this group. The teeth of the South Pyrenean Abelisauridae indet. 1, 2 and 3 morphotypes and the tooth (MON-T10 1) from the Montrebei locality (lower Maastrichtian, chron C31r according to Fondevilla et al., 2019) (Lleida, Spain), assigned to Theropoda indet. by Torices et al. (2015), were later reassigned to cf. *Arcovenator* (Pérez-García et al., 2016) and subsequently to a probable indeterminate abelisaurid (Isasmendi et al., 2022). As discussed above, the differences found between the Abelisauridae indet. 1, 2 and 3 morphotypes from the uppermost Maastrichtian sites of Blasi 1, 2B and 3 and 172-i/04/e (chrons C30n and C29r, Pérez-Pueyo et al., 2021a) (Huesca, Spain) and the teeth of *Arcovenator* indicate that all these tooth morphotypes belong to an abelisaurid other than *Arcovenator*. MON-T10 1 is here regarded as Abelisauridae indet., pending further studies. Despite the presence of abelisaurid theropods throughout the Campanian–Maastrichtian, therefore, the data gathered to date indicate that the pre-turnover abelisaurid genera are not represented in the post-turnover faunas, disappearing before or during the event, with new abelisaurid(s) occurring in post-turnover deposits, as previously suggested by Isasmendi et al. (2022) (Fig. 8).

Cf. *Richardoestesia*/?*Richardoestesia*/cf. ?*Richardoestesia* teeth are mostly known from Iberian deposits and are rare in French deposits (Isasmendi et al., 2022 and references therein). As regards the shape of these teeth, several differences can be found among them. For instance, at Laño, where an important theropod tooth sample has been recovered (Isasmendi et al., 2022), the lower, more distally curved and labiolingually more compressed cf. *Richardoestesia* teeth (the cf. *Richardoestesia* sp. A morphotype) represent by far the most abundant morphotype, and the teeth of the more elongate, straighter, and less compressed cf. *Richardoestesia* sp. B morphotype are less common. By contrast, in the post-turnover South Pyrenean sites of Huesca (Blasi 2B and Veracruz 1; top of chrons C30n and C29r, respectively, according to Pérez-Pueyo et al., 2021a), only one morphotype has been identified, which resembles the cf. *Richardoestesia* sp. B morphotype from Laño. Admittedly, the specimens of the cf. ?*Richardoestesia* tooth morphotype from Molí de Baró-1 (Lleida, upper Maastrichtian, chron C29r, according to Marmi et al., 2016) are more distally curved and lower. However, the more elongate, straighter, and less compressed morphotype is apparently more abundant in the post-turnover deposits. Hence, these taxa could have also been affected by the intra-Maastrichtian faunal turnover (Fig. 8). Nevertheless, further systematic sampling and studies, in addition to the revision of the *Richardoestesia*-like specimen (IPS 18 372) of Prieto-Márquez et al. (2000) from the L'Abeller (Suterranya-1) locality (Lleida), could shed more light on this potential change.

Cf. *Paronychodon*/?*Paronychodon*/aff. *Paronychodon* teeth are yet to be described from uppermost Cretaceous French deposits (Isasmendi et al., 2022). In Iberia, these and similar morphotypes are present in several localities from the upper Campanian to the upper Maastrichtian (Antunes and Sigogneau-Russell, 1991; Ortega et al., 2015; Torices et al., 2015; Marmi et al., 2016; Isasmendi et al., 2022; this study). Overall, no significant differences can be discerned among the Iberian teeth that would allow them to be classified as different morphotypes. Hence, as they are present in both pre- and post-turnover faunas, these theropods were apparently not affected by the intra-Maastrichtian faunal turnover, reinforcing the conclusions reached by Isasmendi et al. (2022) (Fig. 8).

Paravians are among the most abundant and diverse theropods in the Upper Cretaceous of the Ibero-Armorican domain. These are represented by indeterminate paravians, dromaeosaurids, dromaeosaurines, velociraptorines, troodontids, and avialans found in several sites in Iberia and France (Fig. 8). Non-denticulated paravian teeth (Paraves indet. 1 and 2 in this work) have a wide temporal and biogeographical range (Fig. 8). They are present in pre-turnover faunas, having been recovered from the Iberian Chera and Laño sites, as well as from the French Campanian locality of Champ-Garimond (Gard Department, Languedoc) and the middle Campanian (chron C33n) site of La Neuve (Bouches-du-Rhône Department, Provence) (Garcia et al., 2000). They are also present in Iberian faunas during the turnover (Montrebei and Vicari-4 sites, Lleida Province, both from the lower Maastrichtian, chron C31r,

Fig. 8. Temporal occurrences of the uppermost Cretaceous (middle Campanian–Maastrichtian) theropods from the Ibero-Armorican domain. The chronostratigraphic references are based on Fondevilla et al. (2019) and references therein, and Pérez-Pueyo et al. (2021a). Theropod-bearing sites: 1, Pourrières-Jas Neuf Sud; 2, Laño; 3, Armuña; 4, Pourcieux-Les Tuillières; 5, Chera; 6, Trets-La Boucharde; 7, Vitrolles-La Plaine; 8, Velaux-La Bastide Neuve; 9, Fox-Amphoux; 10, Cruzy; 11, 172-i/04/e; 12, Blasi 1, 2b and 3; 13, La Neuve; 14, Montrebei; 15, Vicari-4; 16, Larra-4; 17, Fons, Fons 0 or Champ-Garimond; 18, Lo Hueco; 19, Suterranya-1; 20, Veracruz-1; 21, Molí de Baró-1; 22, Villespassans-Combebelle; 23, Campagne-sur-Aude-Bellevue; 24, Figuerola-2; 25, Amor-2/3; 26, Fontllonga-6; 27, Peguera-1; 28, Roques-Hautes, 29, Sant Romà d'Abella; 30, Camino de Rin-1; 31, Camino de Rin-2; 32, Camino de Fornons 1; 33, Fornons 3; 34, Cassagnau 1; 35, Villespassans-Castigno. The fossil record of the Upper Cretaceous sites of Aveiro, Taveiro and Viso (Portugal), Quintanilla del Coco (Spain), as well as that of certain French sites (e.g., Marignac-Laspeyres-Cassagnau, Lestaillats and Marsoulas, and other sites in Haute-Garonne; Fontjoncouse-Le Bexen in Aude; Serviers in Gard) is not included, due to the lack of exact temporal calibration of the sites (modified from Fondevilla et al., 2019). Silhouettes courtesy of Scott Hartman.

according to Fondevilla et al., 2016a, 2019) and in post-turnover ecosystems (the Blasi 2B and Larra 4 sites, Huesca Province, upper Maastrichtian, top C30n and C29r, respectively, according to Pérez-Pueyo et al., 2021a; Isasmendi et al., 2022). These morphotypes is also present in the Maastrichtian sites of Aveiro and Taveiro (Isasmendi et al., 2022). The paravian teeth that are more elongated and closer to the conidont morphotype are more abundant in the Maastrichtian deposits of the Western Tremp Syncline, whereas the more curved, lower and ziphodont crowns are less common. This contrasts with the pre-turnover site of Laño, where the latter morphotype is by far the most abundant (Isasmendi et al., 2022) (Fig. 8). Therefore, a subtle impact of the intra-Maastrichtian event can be proposed for these indeterminate paravians, confirmation for which is pending on a larger sample of uppermost Maastrichtian specimens.

Dromaeosaurids are quite abundant and are present in both pre- and post-turnover faunas (Fig. 8). Among the different specimens recovered, two dromaeosaurids were described in the French deposits: *Pyroraptor olympius* (Allain and Taquet, 2000) and *Variraptor mechinorum* (Le Loeuff and Buffetaut, 1998). *Pyroraptor* comes from the middle Campanian site of Trets-La Boucharde (Bouches-du-Rhône Department, Provence). Several Iberian teeth have previously been assigned to this genus (Company et al., 2009; Torices et al., 2015), but these cannot be attributed securely to *Pyroraptor* according to Isasmendi et al. (2022). Often considered a *nomen dubium*, *Variraptor* was described on the basis of the last dorsal vertebra and the sacrum recovered at the upper Campanian–lower Maastrichtian locality of Bastide Neuve in Fox-Amphoux (Var Department, Provence). Furthermore, several remains from the upper Campanian to lower Maastrichtian French localities of Cruzy (Languedoc) and Roques-Hautes (Provence) have been assigned to the same taxon (Chanthasit and Buffetaut, 2009). Even though there is no exact age calibration of these sites, it appears that neither of these genera survived into post-turnover times (Fig. 8). As far as the different dromaeosaurid, dromaeosaurine and velociraptorine teeth and other remains are concerned, the lack of detailed descriptions of most of these French and Iberian specimens precludes a thorough assessment of their affinities (Isasmendi et al., 2022).

Dromaeosauridae indet./?Dromaeosauridae indet./cf. Dromaeosauridae indet. remains have been recovered both in France and in the Iberian Peninsula. In Iberia, these remains come from the Maastrichtian sites of Aveiro and Taveiro (Beira Litoral Region) in Portugal (Antunes and Sigogneau-Russell, 1992), as well as the Spanish localities of Amor 3 (Huesca, upper Maastrichtian, chron C29r, according to Puértolas-Pascual et al., 2018; Pérez-Pueyo et al., 2021a), Chera, Figuerola-2 (Lleida, lower–upper Maastrichtian, chron C31r, according to Torices et al., 2015), Fontllonga-6 (Lleida, upper Maastrichtian, chron C30r, according to Torices et al., 2015), Molí de Baró-1, Montrebei, Laño, and the upper Maastrichtian Quintanilla del Coco (Burgos) (Pol et al., 1992; Torices et al., 2015; Marmi et al., 2016; Isasmendi et al., 2022). In France, dromaeosaurid remains have been reported in the lower Maastrichtian of Campagne-sur-Aude-Bellevue (Aude Department, Languedoc), Champ-Garimond, the upper Campanian–lower Maastrichtian of Cruzy and Fox-Amphoux (Var Department), the upper Maastrichtian Marignac-Laspeyres-Cassagnau area (Haute-Garonne Department, Midi-Pyrénées), and the upper Campanian localities of Villespassans-Combebelle and Villespassans-Castigno (Hérault Department, Languedoc) (Sigé et al., 1997; Laurent et al., 2001, 2002; Laurent, 2003; Chanthasit and Buffetaut, 2009; Buffetaut et al., 2021; Santos Brilhante et al., 2022).

At the upper Campanian–lower Maastrichtian site of Lo Hueco (Cuenca, Spain), two dromaeosaurid morphotypes have been distinguished: Dromaeosaurinae indet. and Velociraptorinae indet. (Ortega et al., 2015), as well as a tentatively identified velociraptorine tibia (Malafaia et al., 2023). A single velociraptorine tooth was described from the upper Maastrichtian locality of Peguera-1 (chrons C31r-C31n according to Vila et al., 2012) (Barcelona, Spain) by Baiano et al. (2014). The exhaustively described teeth appear to suggest differences between pre- and post-turnover morphotypes (Fig. 8). Nevertheless, it is not yet possible to assess the possible identity of the taxa present in each assemblage and their precise affinities, and thus the potential effects the intra-Maastrichtian turnover event had on dromaeosaurids (Isasmendi et al., 2022).

The troodontid fossil record is rather poor, with a single taxon, the jinfengopterygine *Tamarro insperatus*, reported from the uppermost Maastrichtian locality of Sant Romà d'Abella (Lleida, chron C29r) (Sellés et al., 2021), together with several cf. Troodontidae indet. teeth from Aveiro and Taveiro (Antunes and Sigogneau-Russell, 1992). The attribution of the teeth was considered doubtful by Isasmendi et al. (2022). Therefore, it is not currently possible to evaluate whether or not this family was affected by the intra-Maastrichtian faunal turnover.

Regarding other theropod remains, Pereda-Suberbiola et al. (2000) mentioned the presence of a possible indeterminate ornithomimosaur at Laño, and several fossils have been attributed to indeterminate theropods. Some of these consist of isolated theropod remains belonging to small- and medium-sized taxa. More thorough studies of this material could lead to its more specific attribution and hence could help us achieve a better understanding of the effects this event had on theropods.

The avialan theropods from the Upper Cretaceous of Ibero-Armorica are poorly and fragmentarily represented. Several upper Campanian–lower Maastrichtian (pre-turnover) sites from France and Spain have yielded isolated remains allowing the erection of the taxon *Gargantuavis philoinos* (Buffetaut and Le Loeuff, 1998). *Gargantuavis* was interpreted as a large terrestrial bird, nested within Ornithuromorpha, and probably within Ornithurae (Buffetaut and Angst, 2019), although the fragmentary, isolated, and scattered condition of its remains has led to this assignation being widely contested (see Buffetaut and Angst, 2020; Mayr et al., 2020). The holotype, a synsacrum and partial ilia (Buffetaut and Le Loeuff, 1998), comes from the Bellevue locality, dated as early Maastrichtian (C32n.1n according to Fondevilla et al., 2016b). Several other sites have provided fossil material referred to *Gargantuavis*, including Bastide Neuve, Montplo-Nord (Cruzy; Hérault Department), Combebelle, Castigno, and Laño (Buffetaut et al., 1995, 2015, 2019, 2021; Buffetaut and Le Loeuff, 1998; Buffetaut and Angst, 2013, 2016a, 2016b, 2019; Angst et al., 2017). The chronological calibration of these sites is not precise beyond the upper Campanian–lower Maastrichtian, except for Laño, Combebelle and Castigno. It should further be pointed out that cervical vertebrae from Lo Hueco have recently been tentatively referred to large ornithuromorph birds (Ortega et al., 2021). The only fossil belonging to a large bird from the upper Maastrichtian (post-turnover) is the cervical vertebra from Beranuy (Huesca) in the Western Tremp Syncline (Pérez-Pueyo et al., 2021b) (Fig. 1B). This fossil is dated to within magnetochron C29r (Puértolas-Pascual et al., 2018) and has been identified as an unnamed ornithuromorph differing from *Gargantuavis*. This might suggest that large birds were also affected by the intra-Maastrichtian faunal turnover, with two clearly different taxa present in the pre- and post-turnover assemblages (Fig. 8). However, the fragmentary and isolated condition of the fossils urges caution with regard to this conclusion.

The Upper Cretaceous of the Ibero-Armorican domain has also yielded some fossils of enantiornithine birds, but due to their rarity and incompleteness, it is difficult to evaluate whether or not Ibero-

Armorican enantiornithines were affected by the faunal turnover. The pre-turnover enantiornithines are represented by two different-sized taxa: *Martinavis cruzyensis* from the Massecaps site (Cruzy, Hérault Department) and *Castignovolucris sebei* from Castigno (Walker et al., 2007; Buffetaut et al., 2023). As well as these two taxa, both identified based on fragmentary material (a humerus and a coracoid, respectively), additional remains of indeterminate enantiornithines have also been recovered from the lower Maastrichtian of France, including a coracoid and a proximal head of a femur from Massecaps (Buffetaut, 1998), and a tibiotarsus from Bastide Neuve (Buffetaut et al., 2000). The post-turnover record of Enantiornithes is almost non-existent, which makes it difficult to estimate the taxonomic impact of the turnover on this clade (Fig. 8). The only fossil assignable to this group is an incomplete scapula from the upper Maastrichtian site of Cassagnau 1 (Laurent, 2003).

7. Conclusions

The systematic, morphometric, and cladistic studies carried out on a sample of 31 isolated theropod teeth found at different localities from the upper Maastrichtian of the Western Tremp Syncline in the South Pyrenean Basin (NE Iberia) allowed us to distinguish a total of eight tooth morphotypes: Abelisauridae indet. 1, 2 and 3, Dromaeosauridae indet., Paraves indet. 1 and 2, cf. *Paronychodon* sp., and cf. *Richardoestesia* sp. As in other uppermost Cretaceous Ibero-Armorican sites, therefore, the late Maastrichtian theropod fauna of the South Pyrenean Basin consists of a medium- to large-sized abelisaurid (Abelisauridae indet. 1, 2 and 3) and several small-sized coelurosaurians (cf. *Paronychodon*, cf. *Richardoestesia*, Paraves indet. 1 and 2, and Dromaeosauridae indet.). The occurrence of different abelisaurid and non-dromaeosaurid paravian morphotypes may be attributable to pseudoheterodonty.

This study has also led to a slight increase in the recorded theropod palaeobiodiversity in the Western Tremp Syncline from six identified theropod tooth morphotypes to eight, with a minimum of five non-avialan theropods. Furthermore, with the presence of the troodontid *Tamarro* and an ornithuromorph avialan, this palaeobiodiversity increases to seven taxa, indicating high theropod palaeobiodiversity in the Western Tremp Syncline.

The revision of these non-avian theropod remains also allowed us to evaluate the effects of the intra-Maastrichtian faunal turnover (known to have occurred from the early Maastrichtian to the early late Maastrichtian; lower part of C31r to the C30r/C30n boundary). Despite the presence of similar theropod groups prior to, during, and subsequent to the intra-Maastrichtian faunal turnover, some differences can be pointed out. These are: (1) the presence of different abelisaurid and dromaeosaurid taxa; (2) the predominance of more elongate, straighter, and less compressed teeth referred to cf. *Richardoestesia* in post-turnover deposits compared to pre-turnover deposits; (3) a higher proportion of more elongated paravian teeth that are closer to a conidont morphology in post-turnover deposits compared to pre-turnover deposits; (4) the presence of Troodontidae only in post-turnover faunas; and (5) the replacement of large gargantuaviid ornithurines by a different large ornithuromorph taxon after the turnover. Therefore, it seems that theropods too were at least partially affected by the turnover event. Nevertheless, more thorough studies and more complete specimens will be needed to better understand the affinities and palaeobiodiversity of Ibero-Armorican theropods, as well as the details of the changes that occurred during this faunal turnover.

CRediT authorship contribution statement

Erik Isasmendi: Writing – review & editing, Writing – original draft, Visualization, Methodology, Investigation, Formal analysis, Conceptualization. **Manuel Pérez-Pueyo:** Writing – review & editing, Writing – original draft, Visualization, Supervision, Methodology, Investigation, Formal analysis, Data curation, Conceptualization. **Miguel Moreno-Azanza:** Writing – review & editing, Validation, Supervision, Resources, Methodology, Investigation, Formal analysis, Conceptualization. **Antonio Alonso:** Writing – review & editing, Writing – original draft, Validation, Supervision, Investigation, Conceptualization. **Eduardo Puértolas-Pascual:** Writing – review & editing, Writing – original draft, Validation, Supervision, Resources, Project administration, Conceptualization. **Beatriz Bádenas:** Writing – review & editing, Writing – original draft, Validation, Resources, Project administration, Funding acquisition, Conceptualization. **José Ignacio Canudo:** Writing – review & editing, Writing – original draft, Validation, Supervision, Resources, Project administration, Investigation, Funding acquisition, Conceptualization.

Declaration of competing interest

The authors declare that they have no known competing financial interests or personal relationships that could have appeared to influence the work reported in this paper.

Data availability

Data is avalaible at Supplementary material.

Acknowledgments

This work was supported by the Spanish Ministry of Science, Innovation and Universities and the European Regional Development Fund (project PID2021-122612OB-I00, MINECO/FEDER, UE); the Basque Government/Eusko Jaurlaritza (research groups IT418-19 and IT1485-22); the University of the Basque Country (UPV/EHU, group PPG17/05) and the Gobierno de Aragón and ERDF (Group E18. Aragosaurus: Recursos Geológicos y Paleoambientales). Erik Isasmendi is supported by a Ph.D. fellowship of the Basque Government/Eusko Jaurlaritza (PRE_2019_1_0215). Manuel Pérez-Pueyo is supported by a N-3 researcher contract of the Universidad de Zaragoza (PUI/2022-090). Eduardo Puértolas Pascual was supported by a postdoctoral contract (María Zambrano) funded by the Ministry of Universities of the Government of Spain through the Next Generation EU funds of the European Union. We thank Phil J. Currie (University of Alberta) and Howard Gibbins (University of Alberta) and Clive Coy (University of Alberta) for their advice and access to the specimens curated at the Dino Lab at the University of Alberta; Ronan Allain (Muséum National d'Histoire Naturelle) and Nour-Eddine Jalil (Muséum National d'Histoire Naturelle) for providing access to the *Pyroraptor* holotype. We would especially like to thank Xabier Pereda-Suberbiola (Universidad del País Vasco/Euskal Herriko Unibertsitatea) for his helpful advice and all the discussions that greatly improved the quality of the manuscript. We also thank Fernando Muñoz for finding specimen MPZ 2021/223 in the outcrops of Arén, Lope Ezquero for finding specimen MPZ 2017/804 in Serraduy, and Joxeba Larrañaga for discovering the Larra sites (Huesca). We are very grateful to Scott Hartman for letting us use his skeletal diagrams and Rupert Glasgow for the English

revision that highly improved the quality of the manuscript. Special thanks are owed to the editors Eduardo Koutsoukos and Maria Rose Petrizzo, and the referees Christophe Hendrickx and one anonymous reviewer.

References

Allain, R., Taquet, P., 2000. A new genus of Dromaeosauridae (Dinosauria, Theropoda) from the Upper Cretaceous of France. Journal of Vertebrate Paleontology 20 (2), 404–407.

Alonso, A., Canudo, J.I., Fernández-Baldor, F.T., Huerta, P., 2017. Isolated theropod teeth associated with sauropod remains from El Oterillo II (Early Cretaceous) site of Salas de los Infantes (Burgos, Spain). Journal of Iberian Geology 43 (2), 193–215.

Angst, D., Buffetaut, E., Corral, J.C., Pereda-Suberbiola, X., 2017. First record of the Late Cretaceous giant bird *Gargantuavis philoinos* from the Iberian Peninsula. Annales de Paléontologie 103, 135–139.

Antunes, M.T., Sigogneau-Russell, D., 1991. Nouvelles données sur les dinosaures du Crétacé supérieur du Portugal. Comptes Rendus de l'Académie des Sciences II 313, 113–119.

Antunes, M.T., Sigogneau-Russell, D., 1992. La faune de petits dinosaures du Crétacé terminal portugais. Comunicacoes dos Servicos Geologicos de Portugal 78 (1), 49–62.

Ardévol, L., Klimowitz, J., Malagón, J., Nagtegaal, P.J.C., 2000. Depositional sequence response to foreland deformation in the upper Cretaceous of the Southern Pyrenees, Spain. AAPG Bulletin 84, 566–588.

Aurell, M., Torromé, D., Gasca, J.M., Calvín, P., Pérez-Pueyo, M., Parrilla-Bel, J., Medrano-Aguado, E., Martín-Closas, C., Vicente, A., Sierra-Campos, P., Canudo, J.I., 2022. Latest Cretaceous palaeogeographic evolution of northeast Iberia: insights from the Campanian continental Montalbán subbasin (Spain). Earth-Science Reviews 235, 104251.

Averianov, A.O., Sues, H.-D., 2007. A new troodontid (Dinosauria: Theropoda) from the Cenomanian of Uzbekistan, with a review of troodontid records from the territories of the former Soviet Union. Journal of Vertebrate Paleontology 27, 87–98.

Averianov, A., Sues, H.D., 2019. Morphometric analysis of the teeth and taxonomy of the enigmatic theropod *Richardoestesia* from the Upper Cretaceous of Uzbekistan. Journal of Vertebrate Paleontology 39, e1614941.

Baiano, M., Galobart, À., Dalla-Vecchia, F.M., Vila, B., 2014. Aplicación de la microtomografía en el estudio de dientes aislados de dinosaurios terópodos. In: Arreguín-Rodríguez, G., Colmenar, J., Díaz-Berenguer, E., Galán, J., Legardalisarri, A., Parrilla-Bel, J., Puértolas-Pascual, E., Silva-Casal, R. (Eds.), New Insights on Ancient Life. XII Encuentro de Jóvenes Investigadores en Paleontología, Boltaña, pp. 57–59.

Blanco, A., Méndez, J.M., Marmi, J., 2015. The fossil record of the uppermost Maastrichtian Reptile Sandstone (Tremp Formation, northeastern Iberian Peninsula). Spanish Journal of Palaeontology 30, 147–160.

Brusatte, S.L., Carr, T.D., 2016. The phylogeny and evolutionary history of tyrannosauroid dinosaurs. Scientific Reports 6, 20252.

Buffetaut, E., 1998. First evidence of enantiornithine birds from the Upper Cretaceous of Europe: postcranial bones from Cruzy (Hérault, France). Oryctos 1, 127–130.

Buffetaut, E., Angst, D., 2013. New evidence of a giant bird from the Late Cretaceous of France. Geological Magazine 150, 173–176.

Buffetaut, E., Angst, D., 2016a. The giant flightless bird *Gargantuavis philoinos* from the Late Cretaceous of southwestern Europe: a review. New Mexico Museum of Natural History and Science Bulletin 71, 41–50.

Buffetaut, E., Angst, D., 2016b. Pelvic elements of the giant bird *Gargantuavis* from the Upper Cretaceous of Cruzy (southern France), with remarks on pneumatisation. Cretaceous Research 66, 171–176.

Buffetaut, E., Angst, D., 2019. A femur of the Late Cretaceous giant bird *Gargantuavis* from Cruzy (southern France) and its systematic implications. Palaeovertebrata 42 (1), e3.

Buffetaut, E., Angst, D., 2020. *Gargantuavis* is an insular basal ornithurine: a comment on Mayr et al., 2020, 'A well-preserved pelvis from the Maastrichtian of Romania suggests that the enigmatic *Gargantuavis* is neither an ornithurine bird nor an insular endemic'. Cretaceous Research 112, 104438.

Buffetaut, E., Le Loeuff, J., 1998. A new giant ground bird from the Upper Cretaceous of southern France. Journal of the Geological Society 155 (1), 1–4.

Buffetaut, E., Marandat, B., Sigé, B., 1986. Découverte de dents de Deinonychosaures (Saurischia, Theropoda) dans le Crétacé supérieur du Sud de la France. Comptes Rendus de l'Académie des Sciences II 303 (15), 1393–1396.

Buffetaut, E., Le Loeuff, J., Mechin, P., Mechin-Salessy, A., 1995. A large French Cretaceous bird. Nature 377, 110.

Buffetaut, E., Mechin, P., Mechin-Salessy, A., 2000. An archaic bird (Enantiornithes) from the Upper Cretaceous of Provence (southern France). Comptes Rendus de l'Académie des Sciences de Paris IIA 331 (8), 557–561.

Buffetaut, E., Angst, D., Mechin, P., Mechin-Salessy, A., 2015. New remains of the giant bird *Gargantuavis philoinos* from the Late Cretaceous of Provence (south-eastern France). Palaeovertebrata 39, 1–6.

Buffetaut, E., Angst, D., Mechin, P., Mechin-Salessy, A., 2019. A femur of the giant bird *Gargantuavis* from the Late Cretaceous of Var (south-eastern France). Carnets Natures 6, 47–52.

Buffetaut, E., Angst, D., Claude, J., Tong, H., Amoros, A., Boschetto, D., Chenet, J.P., Clavel, D., Maggia, B., Roques, T., Sèbe, S., 2021. Les niveaux à vertébrés fossiles du Crétacé supérieur de Castigno et Combebelle (Villespassans, Hérault): historique et nouvelles découvertes. Carnets Natures 8, 41–55.

Buffetaut, E., Angst, D., Tong, H., 2023. A new enantiornithine bird from Upper Cretaceous non-marine deposits at Villespassans (Hérault, southern France). Annales de Paléontologie 109 (1), 102585.

Canale, J.I., Scanferla, C.A., Agnolin, F.L., Novas, F.E., 2009. New carnivorous dinosaur from the Late Cretaceous of NW Patagonia and the evolution of abelisaurid theropods. Naturwissenschaften 96 (3), 409–414.

Canudo, J.I., 2018. The collection of type fossils of the Natural Science Museum of the University of Zaragoza (Spain). Geoheritage 10, 385–392.

Canudo, J.I., Ruiz-Omeñaca, J.I., 2003. Los restos directos de dinosaurios terópodos (excluyendo Aves) en España. In: Pérez-Lorente, F., Romero Molina, M.M., Rivas, P., Coords (Eds.), Dinosaurios y otros reptiles mesozoicos en España. Ciencias de la Tierra, vol. 26. Universidad de La Rioja, Instituto de Estudios Riojanos, Logroño, pp. 347–373.

Canudo, J.I., Oms, O., Vila, B., Galobart, À., Fondevilla, V., Puértolas-Pascual, E., Sellés, A.G., Cruzado-Caballero, P., Dinarès-Turell, J., Vicens, E., Castanera, D., Company, J., Burrel, L., Estrada, R., Marmi, J., Blanco, A., 2016. The upper Maastrichtian dinosaur fossil record from the southern Pyrenees and its contribution to the topic of the Cretaceous-Palaeogene mass extinction event. Cretaceous Research 57, 540–551.

Carrano, M.T., Sampson, S.D., 2008. The phylogeny of Ceratosauria (Dinosauria: Theropoda). Journal of Systematic Palaeontology 6, 183–236.

Carrano, M.T., Sampson, S.D., Forster, C.A., 2002. The osteology of *Masiakasaurus knopfleri*, a small abelisauroid (Dinosauria: Theropoda) from the Late Cretaceous of Madagascar. Journal of Vertebrate Paleontology 22 (3), 510–534.

Carrano, M.T., Benson, R.B.J., Sampson, S.D., 2012. The phylogeny of Tetanurae (Dinosauria: Theropoda). Journal of Systematic Palaeontology 10 (2), 211–300.

Cau, A., Beyrand, V., Voeten, D.F.A.E., Fernandez, V., Tafforeau, P., Stein, K., Barsbold, R., Tsogtbaatar, K., Currie, P.J., Godefroit, P., 2017. Synchrotron scanning reveals amphibious ecomorphology in a new clade of bird-like dinosaurs. Nature 552, 395–399.

Chanthasit, P., Buffetaut, E., 2009. New data on the Dromaeosauridae (Dinosauria: Theropoda) from the Late Cretaceous of southern France. Bulletin de la Societe Geologique de France 180, 145–154.

Chanvry, E., Deschamps, R., Joseph, P., Puigdefàbregas, C., Poyatos-Moré, M., Serra-Kiel, J., Garcia, D., Teinturier, S., 2018. The influence of intrabasinal tectonics in the stratigraphic evolution of piggyback basin fills: towards a model from the Tremp-Graus-Ainsa Basin (South-Pyrenean Zone, Spain). Sedimentary Geology 377, 34–62.

Codrea, V., Smith, T., Dica, P., Folie, A., Garcia, G., Godefroit, P., Van Itterbeeck, J., 2002. Dinosaur egg nests, mammals and other vertebrates from a new Maastrichtian site of the Hateg Basin (Romania). Comptes Rendus Palevol 1, 173–180.

Codrea, V., Solomon, A., Farcaș, C., Barbu, O., 2013. On some local restricted Maastrichtian environments of the "Hațeg Island" (Transylvania, Romania). Bulletin of the Geological Society of Greece XLVII 82–91.

Company, J., Torices, A., Pereda-Suberbiola, X., Ruiz-Omeñaca, J., 2009. Theropod teeth from the Late Cretaceous of Chera (Valencia, eastern Spain). Journal of Vertebrate Paleontology 29, 81A.

Cope, E.D., 1876. Descriptions of some vertebrate remains from the Fort Union beds of Montana. Proceedings of the Academy of Natural Sciences of Philadelphia 28, 248–261.

Corral, J.C., Pueyo, E.L., Berreteaga, A., Rodríguez-Pintó, A., Sánchez, E., Pereda-Suberbiola, X., 2016. Magnetostratigraphy and lithostratigraphy of the Laño vertebrate-site: implications in the uppermost Cretaceous chronostratigraphy of the Basque-Cantabrian Region. Cretaceous Research 57, 473–489.

Csiki-Sava, Z., Buffetaut, E., Ösi, A., Pereda-Suberbiola, X., Brusatte, S.L., 2015. Island life in the Cretaceous - faunal composition, biogeography, evolution, and extinction of land-living vertebrates on the Late Cretaceous European archipelago. ZooKeys 469, 1–161.

Csiki-Sava, Z., Vremir, M., Vasile, Ş., Brusatte, S.L., Dyke, G., Naish, D., Norell, M.A., Totoianu, R., 2016. The East Side Story-the Transylvanian latest Cretaceous continental vertebrate record and its implications for understanding Cretaceous-Paleogene boundary events. Cretaceous Research 57, 662–698.

Currie, P.J., Azuma, Y., 2006. New specimens, including a growth series, of *Fukuiraptor* (Dinosauria, Theropoda) from the Lower Cretaceous Kitadani Quarry of Japan. Journal of the Paleontological Society of Korea 22 (1), 173–193.

Currie, P.J., Evans, D.C., 2020. Cranial anatomy of new specimens of *Saurornitholestes langstoni* (Dinosauria, Theropoda, Dromaeosauridae) from the Dinosaur Park Formation (Campanian) of Alberta. The Anatomical Record 303 (4), 691–715.

Currie, P.J., Varricchio, D.J., 2004. A new dromaeosaurid from the Horseshoe Canyon Formation (upper Cretaceous) of Alberta, Canada. In: Currie, P.J., Koppelhus, E.B., Shugar, M.A., Wright, J.L. (Eds.), Feathered Dragons: Studies on the Transition from Dinosaurs to Birds. Indiana University Press, Bloomington, Indiana, pp. 112–132.

Currie, P.J., Rigby Jr., J.K., Sloan, R.E., 1990. Theropod teeth from the Judith River Formation of southern Alberta, Canada. In: Carpenter, K., Currie, P.J. (Eds.), Dinosaur Systematics: perspectives and approaches 8. Cambridge University Press, New York, pp. 107–125.

Díez-Canseco, D., Arz, J.A., Benito, M.I., Díaz-Molina, M., Arenillas, I., 2014. Tidal influence in redbeds: a palaeoenvironmental and biochronostratigraphic

reconstruction of the Lower Tremp Formation (South-Central Pyrenees, Spain) around the Cretaceous/Paleogene boundary. Sedimentary Geology 312, 31–49.
Eichenseer, H., 1988. Facies Geology of Late Maastrichtian to Early Eocene Coastal and Shallow Marine Sediments (Tremp-Graus Basin, Northeastern Spain). Universität Tübingen, p. 129 (Unpubl. PhD thesis).
Evans, D.C., Larson, D.W., Currie, P.J., 2013. A new dromaeosaurid (Dinosauria: Theropoda) with Asian affinities from the latest Cretaceous of North America. Naturwissenschaften 100 (11), 1041–1049.
Ezcurra, M., 2017. A new early coelophysoid neotheropod from the Late Triassic of Northwestern Argentina. Ameghiniana 54 (5), 506–538.
Fanti, F., Therrien, F., 2007. Theropod tooth assemblages from the Late Cretaceous Maevarano Formation and the possible presence of dromaeosaurids in Madagascar. Acta Palaeontologica Polonica 52 (1), 155–166.
Farlow, J.O., Brinkman, D.L., Abler, W.L., Currie, P.J., 1991. Size, shape, and serration density of theropod dinosaur lateral teeth. Modern Geology 16 (1–2), 161–198.
Fondevilla, V., Dinarès-Turell, J., Oms, O., 2016a. The chronostratigraphic framework of the South-Pyrenean Maastrichtian succession reappraised: implications for basin development and end-Cretaceous dinosaur faunal turnover. Sedimentary Geology 337, 55–68.
Fondevilla, V., Dinarès-Turell, J., Vila, B., Le Loeuff, J., Estrada, R., Oms, O., Galobart, À., 2016b. Magnetostratigraphy of the Maastrichtian continental record in the Upper Aude Valley (northern Pyrenees, France): placing age constraints on the succession of dinosaur-bearing sites. Cretaceous Research 57, 457–472.
Fondevilla, V., Riera, V., Vila, B., Dinarès-Turell, J., Vicens, E., Gaete, R., Oms, O., Galobart, À., 2019. Chronostratigraphic synthesis of the latest Cretaceous dinosaur turnover in south-western Europe. Earth-Science Reviews 191, 168–189.
Fuentes Vidarte, C., Meijide Calvo, M., Meijide Fuentes, F., Meijide Fuentes, M., 2016. Un nuevo dinosaurio estiracosterno (Ornithopoda: Ankylopollexia) del Cretácico Inferior de España. Spanish Journal of Palaeontology 31 (2), 407–446.
Garcia, G., Duffaud, S., Feist, M., Marandat, B., Tambareau, Y., Villatte, J., Sigé, B., 2000. La Neuve, gisement à plantes, invertébrés et vertébrés du Bégudien (Sénonien supérieur continental) du bassin d'Aix-en-Provence. Geodiversitas 22 (3), 325–348.
Gerke, O., Wings, O., 2016. Multivariate and cladistic analyses of isolated teeth reveal sympatry of theropod dinosaurs in the Late Jurassic of Northern Germany. PLoS One 11 (7), e0158334.
Gianechini, F.A., Makovicky, P.J., Apesteguía, S., 2011a. The teeth of the unenlagiine theropod *Buitreraptor* from the Cretaceous of Patagonia, Argentina, and the unusual dentition of the Gondwanan dromaeosaurids. Acta Palaeontologica Polonica 56, 279–290.
Gianechini, F.A., Agnolín, F.L., Ezcurra, M.D., 2011b. A reassessment of the purported venom delivery system of the bird-like raptor *Sinornithosaurus*. Paläontologische Zeitschrift 85, 103–107.
Goloboff, P.A., Catalano, S.A., 2016. TNT version 1.5, including a full implementation of phylogenetic morphometrics. Cladistics 32 (3), 221–238.
Hammer, Ø., Harper, D.A.T., Ryan, P.D., 2001. PAST: paleontological statistics software package for education and data analysis. Palaeontologia Electronica 4 (1), 1–9.
Hendrickx, C., 2015. Evolution of Teeth and Quadrate in Non-avian Theropoda (Dinosauria: Saurischia), with the Description of *Torvosaurus* Remains from Portugal (Unpubl. PhD thesis). Universidade Nova de Lisboa, p. 646.
Hendrickx, C., Mateus, O., 2014. Abelisauridae (Dinosauria: Theropoda) from the Late Jurassic of Portugal and dentition-based phylogeny as a contribution for the identification of isolated theropod teeth. Zootaxa 3759 (1), 1–74.
Hendrickx, C., Mateus, O., Araújo, R., 2015a. A proposed terminology of theropod teeth (Dinosauria, Saurischia). Journal of Vertebrate Paleontology 35 (5), 1–18.
Hendrickx, C., Mateus, O., Araújo, R., 2015b. The dentition of megalosaurid theropods. Acta Palaeontologica Polonica 60 (3), 627–642.
Hendrickx, C., Mateus, O., Araújo, R., Choiniere, J., 2019. The distribution of dental features in non-avian theropod dinosaurs: taxonomic potential, degree of homoplasy, and major evolutionary trends. Paleontologia Electronica 22 (3.74), 1–110.
Hendrickx, C., Tschopp, E., Ezcurra, M., 2020. Taxonomic identification of isolated theropod teeth: the case of the shed tooth crown associated with *Aerosteon* (Theropoda: Megaraptora) and the dentition of Abelisauridae. Cretaceous Research 108, 104312.
Hocknull, S.A., White, M.A., Tischler, T.R., Cook, A.G., Calleja, N.D., Sloan, T., Elliott, D.A., 2009. New mid-Cretaceous (latest Albian) dinosaurs from Winton, Queensland, Australia. PLoS One 4 (7), e6190.
Isasmendi, E., Torices, A., Canudo, J.I., Pereda-Suberbiola, X., 2021. Abelisaurid dinosaurs from the Upper Cretaceous Laño site (Iberian Peninsula). Ciências da Terra Pocedia 1, 38–41.
Isasmendi, E., Torices, A., Canudo, J.I., Currie, P.J., Pereda-Suberbiola, X., 2022. Upper Cretaceous European theropod palaeobiodiversity, paleobiogeography and the intra-Maastrichtian faunal turnover: new contributions from the Iberian fossil site of Laño. Papers in Palaeontology 8 (1), e1419.
Larson, D.W., 2008. Diversity and variation of theropod dinosaur teeth from the uppermost Santonian Milk River Formation (Upper Cretaceous), Alberta: a quantitative method supporting identification of the oldest dinosaur tooth assemblage in Canada. Canadian Journal of Earth Sciences 45 (12), 1455–1468.
Larson, D.W., Currie, P.J., 2013. Multivariate analyses of small theropod dinosaur teeth and implications for paleoecological turnover through time. PLoS One 8 (1), e54329.
Laurent, Y., 2003. Strata (ser 2). Les faunes de vertébrés continentaux du Maastrichtien supérieur d'Europe: systématique et biodiversité, vol. 41, pp. 1–81.
Laurent, Y., Le Loeuff, J., Bilotte, M., Buffetaut, E., Odin, G.S., 2001. Campanian-Maastrichtian continental-marine connection in the Aquitaine-Pyrenees-Provence area (S France). The Campanian-Maastrichtian stage boundary. Elsevier, Amsterdam, pp. 657–665.
Laurent, Y., Bilotte, M., Le Loeuff, J., 2002. Late Maastrichtian continental vertebrates from southwestern France: correlation with marine fauna. Palaeogeography, Palaeoclimatology, Palaeoecology 187, 121–135.
Leymerie, A., 1868. Présence de Garumnien en Espagne. Bulletin de la Société Géologique de France. Bulletin de la Societe Geologique de France 25, 906–911.
Le Loeuff, J., 1992. Les vertébrés continentaux du Crétacé supérieur d'Europe: paléoécologie, biostratigraphie et paléobiogéographie. Mémoires des Sciences de la Terre, Université Pierre and Marie Curie, Paris, p. 273.
Le Loeuff, J., Buffetaut, E., 1991. *Tarascosaurus salluvicus* nov. gen., nov. sp., dinosaure théropode du Crétacé supérieur du Sud de la France. Geobios 24, 585–594.
Le Loeuff, J., Buffetaut, E., 1998. A new dromaeosaurid theropod from the Upper Cretaceous of southern France. Oryctos 1, 105–112.
Le Loeuff, J., Buffetaut, E., Martin, M., 1994. The last stages of dinosaur faunal history in Europe: a succession of Maastrichtian dinosaur assemblages from the Corbières (southern France). Geological Magazine 131, 625–630.
Longrich, N., 2008. Small theropod teeth from the Lance Formation of Wyoming, USA. In: Sankey, J.T., Baszio, S. (Eds.), Vertebrate microfossil assemblages: their role in paleoecology and paleobiogeography. Indiana University Press, Bloomington, Indiana, pp. 135–158.
Longrich, N.R., Pereda-Suberbiola, X., Jalil, N.E., Khaldoune, F., Jourani, E., 2017. An abelisaurid from the latest Cretaceous (late Maastrichtian) of Morocco, North Africa. Cretaceous Research 76, 40–52.
López-Martínez, N., Vicens, E., 2012. A new peculiar dinosaur egg, *Sankofa pyrenaica* oogen. nov. oosp. nov. from the Upper Cretaceous coastal deposits of the Aren Formation, south-central Pyrenees, Lleida, Catalonia, Spain. Palaeontology 55, 325–339.
López-Martínez, N., Canudo, J.I., Ardevol, L., Pereda-Suberbiola, X., Orue-Etxebarria, X., Cuenca-Bescós, G., Ruiz-Omeñaca, J.I., Murelaga, X., Feist, M., 2001. New dinosaur sites correlated with upper Maastrichtian pelagic deposits in the Spanish Pyrenees: implications for the dinosaur extinction. Cretaceous Research 22, 41–61.
Lü, J., Xu, L., Liu, Y., Zhang, X., Jia, S., Ji, Q., 2010. A new troodontid theropod from the Late Cretaceous of central China, and the radiation of Asian troodontids. Acta Palaeontologica Polonica 55, 381–388.
Makovicky, P.J., Norell, M.A., Clark, J.M., Rowe, T., 2003. Osteology and relationships of *Byronosaurus jaffei* (Theropoda: Troodontidae). American Museum Novitates 3402, 1–32.
Malafaia, E., Mocho, P., Escaso, F., Ortega, F., 2017. New data on the anatomy of *Torvosaurus* and other remains of megalosauroid (Dinosauria, Theropoda) from the Upper Jurassic of Portugal. Journal of Iberian Geology 43 (1), 33–59.
Malafaia, E., Escaso, F., Coria, R.A., Ortega, F., 2023. An eudromaeosaurian theropod from Lo Hueco (Upper Cretaceous. Central Spain). Diversity 15, 141.
Marmi, J., Blanco, A., Fondevilla, V., Dalla Vecchia, F.M., Sellés, A.G., Vicente, A., Martín-Closas, C., Oms, O., Galobart, À., 2016. The Molí del Baró-1 site, a diverse fossil assemblage from the uppermost Maastrichtian of the southern Pyrenees (north-eastern Iberia). Cretaceous Research 57, 519–539.
Mayr, G., Codrea, V., Solomon, A., Bordeianu, M., Smith, T., 2020. A well-preserved pelvis from the Maastrichtian of Romania suggests that the enigmatic *Gargantuavis* is neither an ornithurine bird nor an insular endemic. Cretaceous Research 106, 104271.
Meso, J.G., Hendrickx, C., Baiano, M.A., Canale, J.I., Salgado, L., Diaz-Martinez, I., 2021. Isolated theropod teeth associated with a sauropod skeleton from the Late Cretaceous Allen Formation of Río Negro, Patagonia, Argentina. Acta Palaeontologica Polonica 66 (2), 409–423.
Mey, P.H.W., Nagtegaal, P.J.C., Roberti, K.J., Hartevelt, J.J.A., 1968. Lithostratigraphic subdivision of Post-Hercynian deposits in the South-Central Pyrenees, Spain. Leidse Geologische Mededelingen 41, 221–228.
Molnar, R.E., Obata, I., Tanimoto, M., Matsukawa, M., 2009. A tooth of *Fukuiraptor* aff. *F. kitadaniensis* from the Lower Cretaceous Sebayashi Formation, Sanchu Cretaceous, Japan. Bulletin of Tokyo Gakugei University, Division of Natural Sciences 61, 105–117.
Müller, R.T., Langer, M.C., Bronzati, M., Pacheco, C.P., Cabreira, S.F., Dias-Da-Silva, S., 2018. Early evolution of sauropodomorphs: anatomy and phylogenetic relationships of a remarkably well-preserved dinosaur from the Upper Triassic of southern Brazil. Zoological Journal of the Linnean Society 184 (4), 1187–1248.
Muñoz, J.A., 1992. Evolution of a continental collision belt: ECORS-Pyrenees crustal balanced cross-section. In: McClay, K.R. (Ed.), Thrust Tectonics. Springer, Netherlands, Dordrecht, pp. 235–246.
Muñoz, J.A., Mencos, J., Roca, E., Carrera, N., Gratacós, O., Ferrer, O., Fernaández, O., 2018. The structure of the South-Central-Pyrenean fold and thrust belt as constrained by subsurface data. Geológica Acta 16, 439–460.
Mutti, E., Sgavetti, M., 1987. Sequence stratigraphy of the Upper Cretaceous Aren strata in the Aren-Orcau region, south-central Pyrenees, Spain: distinction between eustatically and tectonically controlled depositional sequences. Annali dell'Universita di Ferrara 1, 1–22.
Nagtegaal, P.J.C., Van Vliet, A., Brouwer, J., 1983. Syntectonic coastal offlap and concurrent turbidite deposition: the Upper Cretaceous Aren sandstone in the south-central Pyrenees, Spain. Sedimentary Geology 34, 185–218.

Nessov, L.A., 1995. Dinosaurs of northern Eurasia: new data about assemblages, ecology and paleobiogeography. University of St. Petersburg, St. Petersburg, p. 156 (in Russian).
Novas, F.E., Bandyopadhyay, S., 2001. Abelisaurid pedal unguals from the Late Cretaceous of India. In: VII° International Symposium on Mesozoic Terrestrial Ecosystems, vol. 7. Asociación Paleontológica Argentina, Publicación Especial, pp. 145–149.
Novas, F.E., Pol, D., Canale, J.I., Porfiri, J.D., Calvo, J.O., 2009. A bizarre Cretaceous theropod dinosaur from Patagonia and the evolution of Gondwanan dromaeosaurids. Proceedings of the Royal Society B: Biological Sciences 276, 1101–1107.
Novas, F.E., Agnolín, F.L., Ezcurra, M.D., Porfiri, J., Canale, J.I., 2013. Evolution of the carnivorous dinosaurs during the Cretaceous: the evidence from Patagonia. Cretaceous Research 45, 174–215.
Oms, O., Fondevilla, V., Riera, V., Marmi, J., Vicens, E., Estrada, R., Vila, B., 2016. Transitional environments of the lower Maastrichtian South-Pyrenean Basin (Catalonia, Spain): the Fumanya Member tidal flat. Cretaceous Research 57, 428–442.
Ortega, F., Bardet, N., Barroso-Barcenilla, F., Callapez, P.M., Cambra-Moo, O., Daviero-Gómez, V., Díez Díaz, V., Domingo, L., Elvira, A., Escaso, F., García-Oliva, M., Gómez, B., Houssaye, A., Knoll, F., Marcos-Fernández, F., Martín, M., Mocho, P., Narváez, I., Pérez-García, A., Peyrot, D., Segura, M., Serrano, H., Torices, A., Vidal, D., Sanz, J.L., 2015. The biota of the Upper Cretaceous site of Lo Hueco (Cuenca, Spain). Journal of Iberian Geology 41 (1), 83–99.
Ortega, F., Escaso, F., Malafaia, E., Coria, R.A., 2021. Aves gigantes en al Cretácico Superior de Lo Hueco (Fuentes, Cuenca). In: Proceedings of the Lucas Mallada 23, Libro de Resúmenes de las XXXVI Jornadas de la Sociedad Española de Paleontología, Huesca, Spain, 29 September-2 October 2021, pp. 207–208.
Ősi, A., Apesteguía, S., Kowalewski, M., 2010. Non-avian theropod dinosaurs from the early Late Cretaceous of Central Europe. Cretaceous Research 31 (3), 304–320.
Ősi, A., Szabó, M., Kollmann, H., Wagreich, M., Kalmár, R., Makádi, L., Szentesi, Z., Summesberger, H., 2019. Vertebrate remains from the Turonian (Upper Cretaceous) Gosau Group of Gams, Austria. Cretaceous Research 99, 190–208.
Park, E.J., 2000. Early Cretaceous dinosaur teeth of Korea. Journal of the Paleontological Society of Korea Special Publication 4, 85–98.
Pereda-Suberbiola, X., Astibia, H., Murelaga, X., Elorza, J.J., Gómez-Alday, J.J., 2000. Taphonomy of the Late Cretaceous dinosaur-bearing beds of the Laño Quarry (Iberian Peninsula). Palaeogeography, Palaeoclimatology, Palaeoecology 157 (3), 247–275.
Pereda-Suberbiola, X., Canudo, J.I., Cruzado-Caballero, P., Barco, J.L., López-Martínez, N., Oms, O., Ruiz-Omeñaca, J.I., 2009. The last hadrosaurid dinosaurs of Europe: a new lambeosaurine from the Uppermost Cretaceous of Aren (Huesca, Spain). Comptes Rendus Palevol 8, 559–572.
Pérez-García, A., Ortega, F., Bolet, A., Escaso, F., Houssaye, A., Martínez-Salanova, J., Chaves, C.M., Mocho, P., Narváez, I., Segura, M., Torices, A., Vidal, D., Sanz, J.L., 2016. A review of the upper Campanian vertebrate site of Armuña (Segovia Province, Spain). Cretaceous Research 57, 591–623.
Pérez-Pueyo, M., Puértolas-Pascual, E., Canudo, J.I., Bádenas, B., 2019. Larra 4: desenterrando a los últimos vertebrados del Maastrichtiense terminal del Pirineo aragonés. Zubía, Volumen Especial 31, 175–180.
Pérez-Pueyo, M., Cruzado-Caballero, P., Moreno-Azanza, M., Vila, B., Castanera, D., Gasca, J.M., Puértolas-Pascual, E., Bádenas, B., Canudo, J.I., 2021a. The Tetrapod Fossil Record from the Uppermost Maastrichtian of the Ibero-Armorican Island: an Integrative Review Based on the Outcrops of the Western Tremp Syncline (Aragón, Huesca Province, NE Spain). Geosciences 11 (4), 162.
Pérez-Pueyo, M., Puértolas-Pascual, E., Moreno-Azanza, M., Cruzado-Caballero, P., Gasca, J.M., Núñez-Lahuerta, C., Canudo, J.I., 2021b. First record of a giant bird (Ornithuromorpha) from the uppermost Maastrichtian of the Southern Pyrenees, northeast Spain. Journal of Vertebrate Paleontology, e1900210.
Pol, C., Buscalioni, A.D., Carballeira, J., Frances, V., López- Martínez, N., Marandat, B., Moratalla, J.J., Sanz, J.L., Sigé, B., Villatte, J., 1992. Reptiles and mammals from the Late Cretaceous new locality Quintanilla del Coco (Burgos province, Spain). Neues Jahrbuch für Geologie und Paläontologie - Abhandlungen 184, 279–314.
Prieto-Márquez, A., Gaete, R., Galobart, A., Ardévol, L., 2000. A *Richardoestesia*-like theropod tooth from the Late Cretaceous foredeep, south-central Pyrenees, Spain. Eclogae Geologicae Helvetiae 93 (3), 497–502.
Puértolas-Pascual, E., Arenillas, I., Arz, J.A., Calvín, P., Ezquerro, L., García-Vicente, C., Pérez-Pueyo, M., Sánchez-Moreno, E.M., Villalaín, J.J., Canudo, J.I., 2018. Chronostratigraphy and new vertebrate sites from the upper Maastrichtian of Huesca (Spain), and their relation with the K/Pg boundary. Cretaceous Research 89, 36–59.
Rasband, W.S., 2003. Image J [WWW Document]. National Institutes of Health, Bethesda, Maryland, USA. Online version at: http://rsb.info.nih.gov/ij/.
Rauhut, O.W.M., Carrano, M.T., 2016. The theropod dinosaur *Elaphrosaurus bambergi* Janensch, 1920, from the Late Jurassic of Tendaguru, Tanzania. Zoological Journal of the Linnean Society 178 (3), 546–610.
Rauhut, O.W.M., Foth, C., Tischlinger, H., Norell, M.A., 2012. Exceptionally preserved juvenile megalosauroid theropod dinosaur with filamentous integument from the Late Jurassic of Germany. Proceedings of the National Academy of Sciences 109 (29), 11746–11751.
Rauhut, O.W.M., Hübner, T., Lanser, K.-P., 2016. A new megalosaurid theropod dinosaur from the late Middle Jurassic (Callovian) of north-western Germany: implications for theropod evolution and faunal turnover in the Jurassic. Palaeontologia Electronica 19 (2), 1–65.
Riera, V., Oms, O., Gaete, R., Galobart, À., 2009. The end-Cretaceous dinosaur succession in Europe: the Tremp Basin record (Spain). Palaeogeography, Palaeoclimatology, Palaeoecology 283, 160–171.
Rosell, J., Linares, R., Llompart, C., 2001. El "garumniense" prepirenaico. Revista de la Sociedad Geologica de Espana 14, 47–56.
Sankey, J.T., 2008. Diversity of Latest Cretaceous (Late Maastrichtian) small theropods and birds: teeth from the Lance and Hell Creek Formations, USA. In: Sankey, J.T., Baszio, S. (Eds.), Vertebrate microfossil assemblages: Their role in paleoecology and paleobiogeography. Indiana University Press, pp. 117–134.
Sankey, J.T., Brinkman, D.B., Guenther, M., Currie, P.J., 2002. Small theropod and bird teeth from the Late Cretaceous (Late Campanian) Judith River Group, Alberta. Journal of Paleontology 76, 751–763.
Sankey, J.T., Standhardt, B.R., Schiebout, J.A., 2005. Theropod teeth from the Upper Cretaceous (Campanian-Maastrichtian), Big Bend National Park, Texas. In: Carpenter, K. (Ed.), The carnivorous dinosaurs. Indiana University Press, pp. 127–152.
Santos Brilhante, N., de França, T.C., Castro, F., Sanches da Costa, L., Currie, P.J., Kugland de Azevedo, S.A., Delcourt, R., 2022. A dromaeosaurid-like claw from the Upper Cretaceous of southern France. Historical Biology 34 (11), 2195–2204.
Sellés, A.G., Vila, B., Galobart, À., 2014. Diversity of theropod ootaxa and its implications for the latest Cretaceous dinosaur turnover in South-Western Europe. Cretaceous Research 49, 45–54.
Sellés, A.G., Vila, B., Brusatte, S.L., Currie, P.J., Galobart, A., 2021. A fast-growing basal troodontid (Dinosauria: Theropoda) from the latest Cretaceous of Europe. Scientific Reports 11, 4855.
Sereno, P.C., 1997. The origin and evolution of dinosaurs. Annual Review of Earth and Planetary Sciences 25 (1), 435–489.
Sereno, P.C., Brusatte, S.L., 2008. Basal abelisaurid and carcharodontosaurid theropods from the Lower Cretaceous Elrhaz Formation of Niger. Acta Palaeontologica Polonica 53 (1), 15–46.
Serra-Kiel, P., Canudo, J., Dinares, J., Molina, E., Ortiz, N., Pascual, J., Samso, J., Tosquella, J., 1994. Cronoestratigrafía de los sedimentos marinos del Terciario inferior de la Cuenca de Tremp-Graus (Zona Central Surpirenaica). Revista de la Sociedad Española de Geología 7, 273–299.
Sibuet, J.-C., Srivastava, S.P., Spakman, W., 2004. Pyrenean orogeny and plate kinematics. Journal of Geophysical Research: Solid Earth 109 (B08104).
Sigé, B., Buscalioni, A.D., Duffaud, S., Gayet, M., Orth, B., Rage, J.C., Sanz, J.L., 1997. Etat des données sur le gisement crétacé supérieur continental de Champ-Garimond (Gard, Sud de la France). Münchner Geowissenschaftliche Abhandlungen 34, 111–130.
Smith, J.B., 2005. Heterodonty in *Tyrannosaurus rex*: implications for the taxonomic and systematic utility of theropod dentitions. Journal of Vertebrate Paleontology 25 (4), 865–887.
Smith, J.B., 2007. Dental morphology and variation in *Majungasaurus crenatissimus* (Theropoda: Abelisauridae) from the Late Cretaceous of Madagascar. Journal of Vertebrate Paleontology 27 (S2), 103–126.
Smith, J.B., Lamanna, M.C., 2006. An abelisaurid from the Late Cretaceous of Egypt: implications for theropod biogeography. Naturwissenschaften 93 (5), 242–245.
Smith, J.B., Vecchia, F.M.D., 2006. An abelisaurid (Dinosauria: Theropoda) tooth from the Lower Cretaceous Chicla Formation of Libya. Journal of African Earth Sciences 46 (3), 240–244.
Smith, T., Codrea, V., Săsăran, E., Van Itterbeck, J., Bultynck, P., Csiki, Z., Dica, P., Fărcaş, C., Folie, A., Garcia, G., Godefroit, P., 2002. A new exceptional vertebrate site from the Late Cretaceous of the Haţeg Basin (Romania). Studia Universitatis Babeş-Bolyai. Geologia Special issue 1, 321–330.
Smith, J.B., Vann, D.R., Dodson, P., 2005. Dental morphology and variation in theropod dinosaurs: implications for the taxonomic identification of isolated teeth. The Anatomical Record Part A: Discoveries in Molecular, Cellular, and Evolutionary Biology: An Official Publication of the American Association of Anatomists 285 (2), 699–736.
Sues, H.-D., Averianov, A.O., 2013. Enigmatic teeth of small theropod dinosaurs from the Upper Cretaceous (Cenomanian-Turonian) of Uzbekistan. Canadian Journal of Earth Sciences 50 (3), 306–314.
Teixell, A., 1998. Crustal structure and orogenic material budget in the west central Pyrenees. Tectonics 17, 395–406.
Torices, A., 2007. Los dinosaurios terópodos del Cretácico Superior de la Cuenca Surpirenaica. Universidad Complutense de Madrid, p. 409 (Unpubl. PhD thesis).
Torices, A., Currie, P.J., Canudo, J.I., Pereda-Suberbiola, X., 2015. Theropod Dinosaurs from the Upper Cretaceous of the South Pyrenees Basin of Spain. Acta Palaeontologica Polonica 60, 611–626.
Tortosa, T., Buffetaut, E., Vialle, N., Dutour, Y., Turini, E., Cheylan, G., 2014. A new abelisaurid dinosaur from the Late Cretaceous of southern France: palaeobiogeographical implications. Annales de Paléontologie 100 (1), 63–86.
Tsuihiji, T., Barsbold, R., Watabe, M., Tsogtbaatar, K., Chinzorig, T., Fujiyama, Y., Suzuki, S., 2014. An exquisitely preserved troodontid theropod with new information on the palatal structure from the Upper Cretaceous of Mongolia. Naturwissenschaften 101, 131–142.
Ullastre, J., Masriera, A., 1998. Nuevas aportaciones al conocimiento estratigráfico del Paleoceno continental del Pirineo catalán (España). Treballs del Museu de Geologia de Barcelona 7, 95–128.
Valentin, X., Godefroit, P., Tabuce, R., Vianey-Liaud, M., Wu, W., García, G., 2012. First late Maastrichtian (latest Cretaceous) vertebrate assemblage from Provence

(Vitrolles-la-Plaine, southern France). In: Godefroit, P. (Ed.), Bernissart Dinosaurs and Early Cretaceous Terrestrial Ecosystems. Indiana University Press, Bloomington, pp. 582–597.
Vasile, Ş., 2008. A new microvertebrate site from the Upper Cretaceous (Maastrichtian) deposits of the Haţeg Basin. Sargetia 21, 5–15.
Vasile, Ş., Grigorescu, D., Csiki-Sava, Z., 2012. Maastrichtian continental microvertebrates from Fărcădeana (Rusca Montană Basin, Romania). In: Royo-Torres, R., Gascó, F., Alcalá, L. (Eds.), 10th Annual Meeting of the European Association of Vertebrate Palaeontologists, Teruel (Spain), June 2012, Fundamental, vol. 20, pp. 271–273.
Vicente, A., Martín-Closas, C., Arz, J.A., Oms, O., 2015. Maastrichtian–basal Paleocene charophyte biozonation and its calibration to the Global Polarity Time Scale in the southern Pyrenees (Catalonia, Spain). Cretaceous Research 52, 268–285.
Vicente, A., Villalba-Breva, S., Ferràndez-Cañadell, C., Martín-Closas, C., 2016. Revision of the Maastrichtian-Palaeocene charophyte biostratigraphy of the Fontllonga reference section (Southern Pyrenees, Catalonia, Spain). Geológica Acta 14, 349–362.
Vila, B., Galobart, À., Canudo, J.I., Le Loeuff, J., Dinarès-Turell, J., Riera, V., Oms, O., Tortosa, T., Gaete, R., 2012. The diversity of sauropods and their first taxonomic succession from the latest Cretaceous of southwestern Europe: clues to demise and extinction. Palaeogeography, Palaeoclimatology, Palaeoecology 350–352, 19–38.
Vila, B., Sellés, A.G., Brusatte, S.L., 2016. Diversity and faunal changes in the latest Cretaceous dinosaur communities of southwestern Europe. Cretaceous Research 57, 552–564.
Walker, C.A., Buffetaut, E., Dyke, G.J., 2007. Large euenantiornithine birds from the Cretaceous of southern France, North America and Argentina. Geological Magazine 144, 977–986.
Wang, S., Stiegler, J., Amiot, R., Wang, X., Du, G., Clark, J.M., Xu, X., 2017. Extreme ontogenetic changes in a ceratosaurian theropod. Current Biology 27 (1), 144–148.
White, M.A., Bell, P.R., Cook, A.G., Poropat, S.F., Elliott, D.A., 2015. The dentary of *Australovenator wintonensis* (Theropoda, Megaraptoridae); implications for megaraptorid dentition. PeerJ 3, e1512.
Williamson, T.E., Brusatte, S.L., 2014. Small theropod teeth from the Late Cretaceous of the San Juan Basin, northwestern New Mexico and their implications for understanding latest Cretaceous dinosaur evolution. PLoS One 9 (4), e93190.
Xu, X., Norell, M.A., 2004. A new troodontid dinosaur from China with avian-like sleeping posture. Nature 431, 838–841.
Young, C.M., Hendrickx, C., Challands, T.J., Foffa, D., Ross, D.A., Butler, I.B., Brusatte, S.L., 2019. New theropod dinosaur teeth from the Middle Jurassic of the Isle of Skye, Scotland. Scottish Journal of Geology 55 (1), 7–19.

Appendix A. Supplementary data

Supplementary data to this article can be found online at https://doi.org/10.1016/j.cretres.2024.105952.